C. R. Chimie 21 (2018) 1209–1229

Contents lists available at ScienceDirect

Comptes Rendus Chimie

www.sciencedirect.com

Account/Revue

Polynuclear Fe(II) complexes: Di/trinuclear molecules and coordination networks

Jose Ramón Galán Mascarós [a, b, **], Guillem Aromí [c, d, *], Mohanad Darawsheh [c]

[a] Institute of Chemical Research of Catalonia (ICIQ), The Barcelona Institute of Science and Technology (BIST), Av. Països Catalans, 16, 43007 Tarragona, Spain
[b] ICREA, Pg. Lluís Companys 23, 08010 Barcelona, Spain
[c] Departament de Química Inorgànica i Orgànica, Universitat de Barcelona, Diagonal 645, 08028 Barcelona, Spain
[d] Institute of Nanoscience and Nanotechnology of the University of Barcelona (IN2UB), Spain

ARTICLE INFO

Article history:
Received 27 November 2017
Accepted 17 July 2018
Available online 23 August 2018

Keywords:
Spin crossover
Iron
Host–guest systems
Molecular devices
Coordination chemistry
Coordination polymers

ABSTRACT

We review here the recent progress made in the synthesis of spin crossover (SCO) Fe(II) coordination complexes with two or three metal atoms, as well as coordination polymers, with the main focus on that in the last five years. We discuss these as well as their magnetic properties to derive magnetostructural correlations. This manuscript is organized through the ligand types that serve to produce the various coordination systems presented. The ligand structure and essential SCO parameters of the complexes are gathered in comprehensive figures and tables. This review illustrates the richness and key parameters of coordination chemistry to develop multiple architectures with the desired properties involving this fascinating phenomenon.

1. Introduction

The phenomenon of spin crossover (SCO) is one of the most appealing strategies towards molecular switches. The reversible transition between two spin states is accompanied by changes in the electronic properties of a molecule/material, from magnetism to spectroscopy or transport. In the case of Fe(II) (d^6), the SCO takes place between a diamagnetic spin state ($S = 0$; low spin, LS) and a paramagnetic spin state ($S = 2$; high spin, HS) [1]. Besides the dramatic impact on the magnetic behavior [2], the transition may lead to radically different optical [3–5], electrical [6–9] or chemical properties [10,11]. In addition, Fe(II) systems experience significant structural changes upon SCO due to the transition from the LS state with only occupied non-bonding orbitals to the HS state with two semi-occupied antibonding orbitals. Therefore, the LS to HS transition causes an elongation of the coordination bonds (usually of 10–12%). Within a crystal lattice, these local structural effects propagate throughout the material and determine the dynamic properties of this transition; if the active SCO centers of the network are strongly connected by extended covalent or intermolecular interactions, the transition will likely be cooperative and may exhibit hysteresis and bistability [12,13]. In part for the above reasons, the vast majority of SCO systems studied are ferrous coordination compounds.

From the historical SCO database, it has become clear that complexes of Fe(II) with a majority of N-donor ligands are prone to exhibit the SCO behavior. Despite the huge number of examples, only a few Fe(II) SCO compounds have been studied in the areas of nano-structuration, advanced spectroscopic studies, guest–host research, etc. This

* Corresponding author. Departament de Química Inorgànica i Orgànica, Universitat de Barcelona, Diagonal 645, 08028 Barcelona, Spain.
** Corresponding author. Institute of Chemical Research of Catalonia (ICIQ), Av. Països Catalans, 16, 43007 Tarragona, Spain.
E-mail addresses: jrgalan@ICIQ.ES (J.R. Galán Mascarós), guillem.aromi@qi.ub.es (G. Aromí).

https://doi.org/10.1016/j.crci.2018.07.005
1631-0748/

List of abbreviations

SCO	spin crossover
LS	low spin
HS	high spin
SCXRD	single crystal X-ray diffraction
SCSC	single crystal to single crystal
DMF	dimethylformamide
^{1}H NMR	proton nuclear magnetic resonance
MS	mass spectrometry
CL	capping ligand
mer	meridional
fac	facial
LIESST	light induced excited spin state trapping
PB	Prussian blue
GM	guest molecule
e.g.	in Latin, *exempli gratia* (for example)
salen	salicylaldehyde/ethylenediamine based ligand
abr.	abrupt
inc.	incomplete
gr.	gradual
2-st and 3-st	two and three steps, respectively
0D, 1D, 2D, and 3D	zero, one, two and three dimensional, respectively

suggests that there is certainly a large amount of fundamental knowledge and the potential applications of this phenomenon are ready to be discovered from the many other compounds available. This shall occur as a consequence of the increased multidisciplinarity that has been developed in recent years.

In this review, the focus is placed on the synthesis of SCO Fe(II) coordination compounds comprising active molecules of two or three metal centers, or coordination polymers, reported since 2012. Another paper of this special issue is consecrated already to mononuclear systems, while a third one focuses on non-ferrous systems. Clusters or polymers of Fe(II) with the SCO behavior published previously to this year have been revised through excellent reviews [14–18].

The special interest in polynuclear compounds is twofold. On the one hand, polynuclear complexes are more prone to exhibit multi-step transitions, because of the easy implementation of crystallographically non-equivalent Fe(II) positions. This can be designed with the help of non-symmetric bridging ligands, for example. Multistep transitions could be the basis for developing multi-state memories, beyond the simple binary system of <1> and <0> states. On the other hand, it is easy to envision how polynuclear compounds (and particularly coordination polymers) allow establishing stronger connectivity between SCO centers. Stronger connectivity typically means enhanced cooperativity, resulting in higher critical temperatures, more abrupt transitions, and the appearance of wide hysteresis cycles. Indeed, most SCO materials with the memory effect above room temperature are polynuclear complexes and coordination polymers.

The present paper is divided by nuclearities (from dinuclear to trinuclear to polymeric), and each block is organized by the type of bridging ligand. A common feature of all the compounds reviewed in this manuscript is the presence of metals coordinatively linked by bridging ligands. All the bridging ligands have been labeled, and their structures are shown in various figures. Very often, the assistance of additional capping ligands becomes necessary to complete the coordination sphere around the metals, to control/determine dimensionality and/or to promote the SCO behavior. The latter are also listed. A list of all SCO complexes featured in this review is given in Table 1, where the main parameters of the magnetic behavior are summarized.

2. Recent results

2.1. Dinuclear complexes

Most discrete Fe(II) coordination compounds showing SCO are mononuclear [19–21]. However, there has been an interest in preparing SCO Fe(II) clusters to probe the synergy or correlation between SCO and intramolecular magnetic exchange in a simple system [22]. In addition, they afford discrete molecules with more than two possible spin registries. In the case of dinuclear systems, these are [LS–LS], [LS–HS] and [HS–HS]. The simplicity of such dinuclear systems also allows computational modeling [23]. In addition, dinuclear Fe(II) SCO molecules have shown the ability to tune the stability of the spin state at one site, via structural modifications on the other site [24].

2.1.1. Complexes with 'N–N'-diazole bridges

Heterocyclic five or six membered rings containing the 'N–N'-diazole moiety are excellent bridging ligands and are found profusely among coordination chemistry compounds (especially the former) [16,25]. Of particular relevance for the topic of SCO is the group of 1,2,4-triazoles (trz, Fig. 1), which gives place to a largely studied family of Fe(II) complexes. Most such triazoles lead to 1D coordination polymers with formula $[Fe(trz)_3]_n(X)_{2n}$ (X^- are counterions; see below) [18]; however, a few discrete Fe/trz complexes have also been reported [16,26]. One of the most interesting precedents is the complex $[Fe_2(L1)_5(NCS)_4]$ (**1**; L1, *N*-salicylidene-4-amino-1,2,4-triazole) [27]. It features two Fe(II) centers bridged by three triazole ligands (L1) and bound to two additional capping L1 donors, with the coordination of each metal completed by two *cis* SCN^- groups. This compound exhibits abrupt SCO centered at $T_{1/2}$ = 150 K, as determined through magnetic measurements and confirmed by Mössbauer spectroscopy. The latter technique showed that the transition between [LS–LS] and [HS–HS] states occurs without the intermediacy of any [LS–HS] phase. Because of the photochromism of L1, complex **1** is fluorescent and the emission is very sensitive to the spin state. Thus, the SCO can be monitored through luminescence measurements. The publication of **1** was followed by reports on a few other derivatives. The structure of the complex $[Fe_2(L2)_5(NCS)_4]$ (**2**, Fig. 2; L2, 4-phenylimino-1,2,4-triazole) [28] is completely analogous. It features incomplete SCO (approximately half of its metal centers)

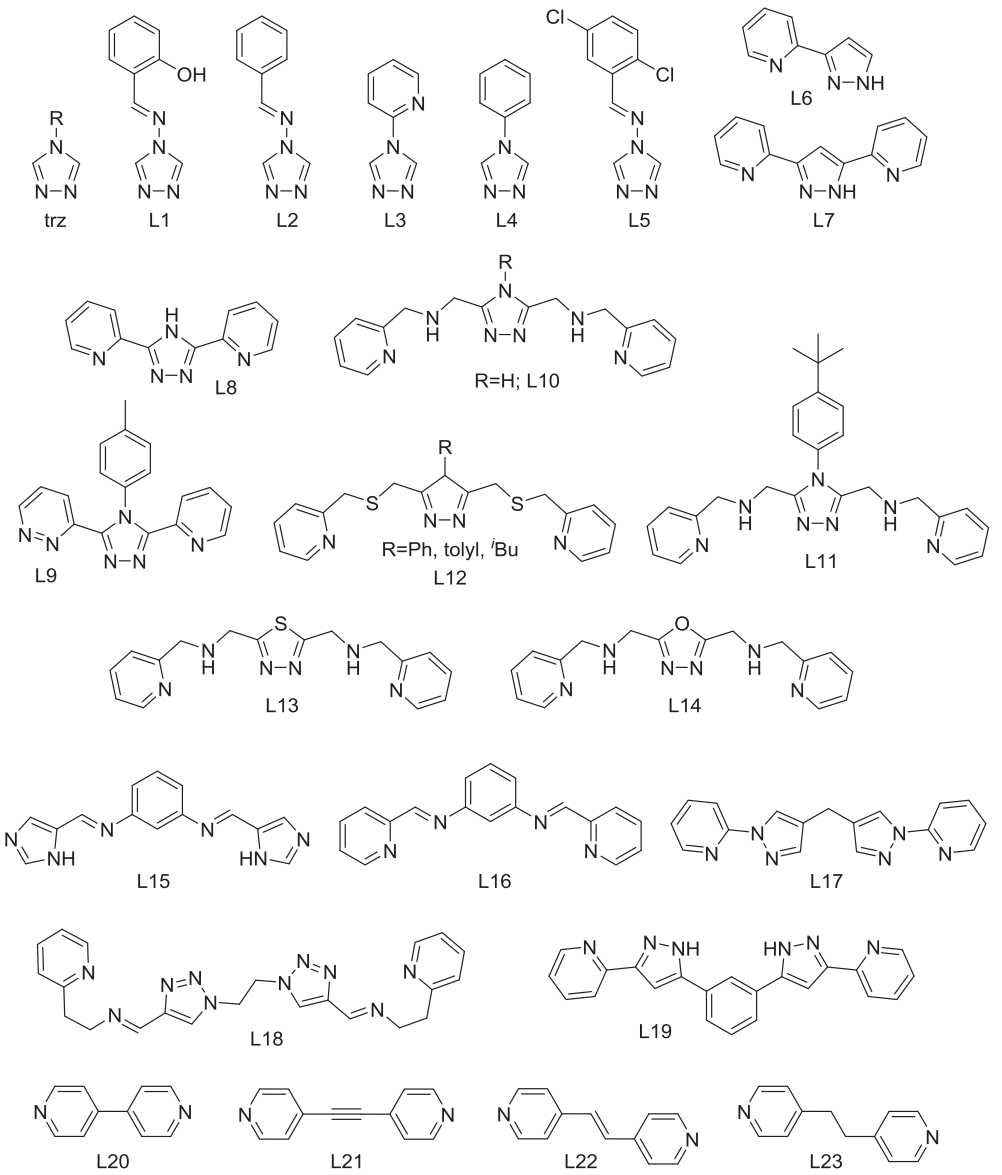

Fig. 1. Structure of bridging ligands mentioned in this review.

with a $T_{1/2}$ value of 115 K. The analysis of the molecular structure at 100 K revealed that all Fe(II) centers exhibit parameters in-between the LS and the HS states, thus suggesting that, at this temperature, the lattice does not contain ordered [LS–HS] entities, but disordered [LS–LS] and [HS–HS] species. If crystals of **2** are left in air, they turn into powder following the exchange of lattice methanol molecules by water. This stabilizes the [HS–HS] for the whole range of temperatures, which allowed determining the intramolecular antiferromagnetic coupling in this series. A similar solvent effect was observed in the analogue $[Fe_2(L3)_5(NCS)_4]$ (**3**; L3, 4-(2-pyridyl)-1,2,4-triazole) [29]. Interestingly, two solvatomorphs were prepared independently by using, respectively, MeOH/EtOH and water as solvents. The former incorporates molecules of MeOH and EtOH in the lattice and exhibits an SCO of 50% of the metal centers. The other derivative features water lattice molecules, and 100% of its iron centers are in the HS state down to 2 K. The interesting difference with **2** is that the mixed-spin compound is now made of ordered [LS–HS] molecules. This behavior was confirmed thoroughly in the new derivative $[Fe_2(L4)_5(NCS)_4]$ (**4**; L4, 4-phenyl-1,2,4-triazole) [30]. The preparation of **4** in ethanol affords the EtOH solvate, also undergoing an SCO of 50% of its iron centers. This solvate exhibits a single crystal to single crystal (SCSC) transformation described as $\mathbf{4}\cdot 2EtOH + 1.5H_2O \rightarrow \mathbf{4}\cdot 2EtOH\cdot 1.5H_2O$, stabilizing the [HS–HS].

As an attempt to correlate the SCO properties with the electronic properties of ligand substituents, the 2,5-dichloro version of L2 (i.e. 2,5-dichloro-4-phenylimino-1,2,4-triazole; L5) was employed to make the complex $[Fe_2(L5)_5(NCS)_4]$ (**5**). Its H_2O solvate was found to exhibit

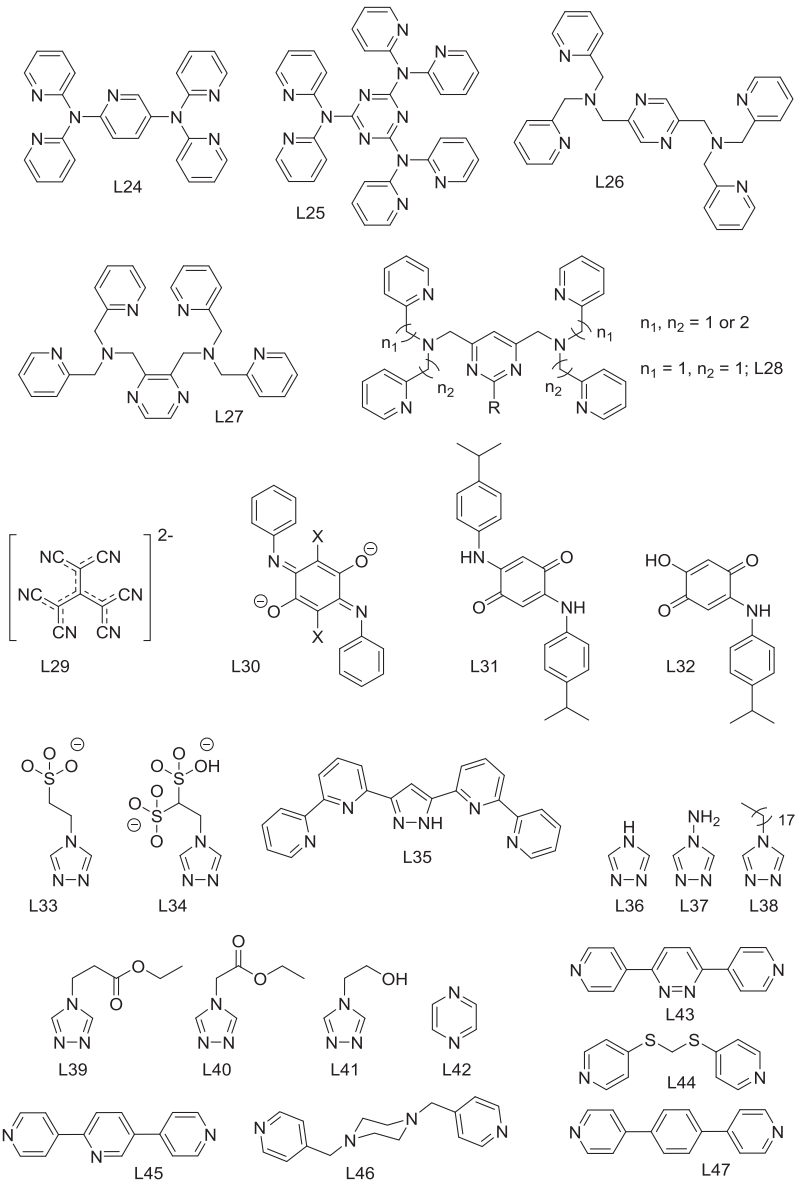

Fig. 1. *(continued)*

complete SCO with a $T_{1/2}$ value 35 K higher (150 K) [31]. This shift was attributed, at least in part to the larger electron withdrawing nature of the substituents, although other effects could play a role.

One strategy for enforcing the formation of discrete dinuclear molecules with 'N–N' bridges from triazole or pyrazole moieties is by incorporating additional coordinating arms into these rings. These ligands, together with XCN^- anions (X = S, Se or BH_3), furnish a suitable recipe for the preparation of SCO dimers [14]. The early examples were made of 3-(2′-pyridyl)-pyrazole (L6) [32] and 3,5-bis-(2′-pyridyl)-pyrazole (L7) [33], and served to characterize for the first time an ordered phase with two components, the [LS–LS] and the [HS–HS], at the intermediate plateau of a two-step SCO [34]. In addition, thanks to the synthetic versatility allowing us to change the neutral terminal ligands that complete the coordination sphere of the metal ions, the SCO temperature could be easily tuned [35]. One of these compounds, $[Fe_2(NCSe)_2(L7)_2(py)_2]$ (**6**) [36], was used to establish a relationship between the lattice at the atomic level and the macroscopic orientation of the LS–HS interface during the thermal transition. It was found that the orientation of this interface is causing the least mismatch between both phases [37].

Of the dinuclear compounds discussed up to now, those with the analogue 3,5-bis-(2′-pyridyl)-1,2,4-triazole (L8) [36], have constituted a suitable basis to predict if the [LS–LS] to [HS–HS] transition can occur directly or through the formation of an ordered intermediate [LS–HS] phase [38]. Very recently, the related asymmetric ligand 3-(2′-

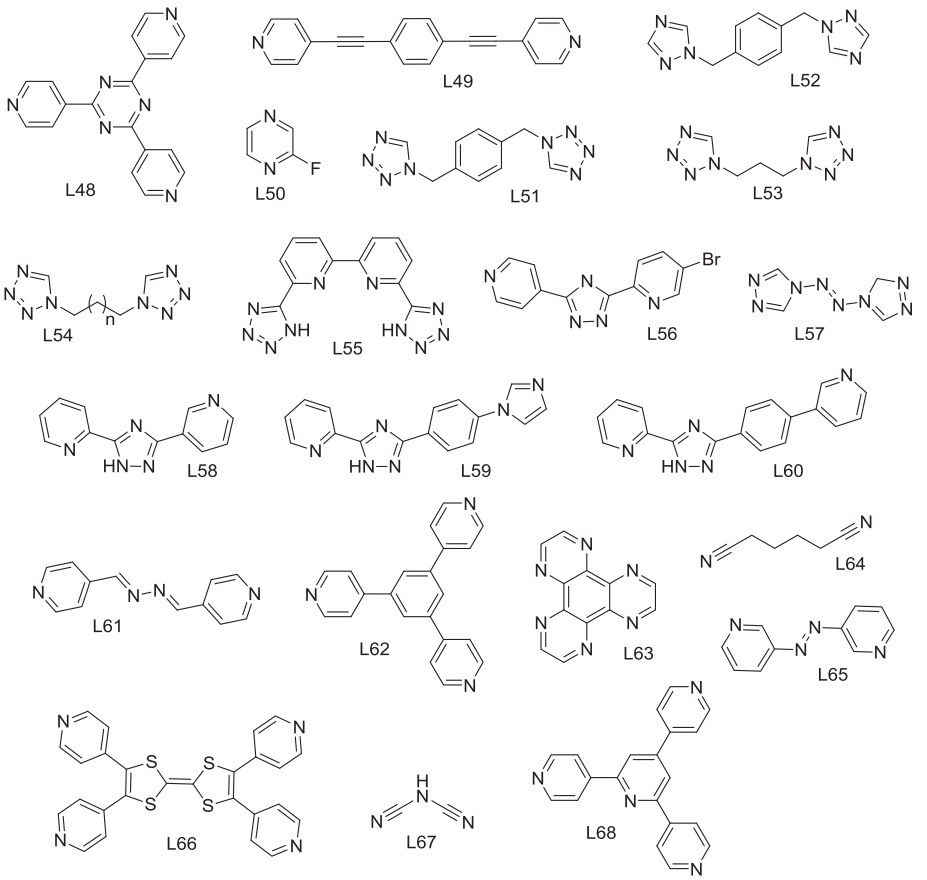

Fig. 1. *(continued)*

pyridyl)-4-(*p*-tolyl)-5-(3′-pyridazine)-1,2,4-triazole (L9) was used to prepare the dinuclear complex $[Fe_2(L9)_2(MeCN)_4](BF_4)_4$ (**7**) [39]. This salt undergoes various solvent exchange processes in form of SCSC transformations, accompanied by changes in the spin state of the Fe(II) ions and therefore, in color. These phenomena convert this system into a candidate for a molecular chemical sensor for small molecules or gases [40]. Thus, exposure of **7** to EtOH transforms it into $[Fe_2(L9)_2(EtOH)_4](BF_4)_4$ (**8**) while the process can be reversed by passing vapors of MeCN. Compound **8** can be transformed into $[Fe_2(L9)_2(H_2O)_4](BF_4)_4$ (**9**) by passing a stream of H_2O. This transformation is more remarkable because **9** is in fact polymeric, as a result of a change in the coordination mode of L9, which turns from μ into μ_3 by rotation of the pyridazine group. This polymerization is reversible by dehydration through heating, followed by exposure to an MeCN atmosphere.

A set of ligands related to L8 and L9 are derived from 3,5-bis-(((2-pyridylmethyl)-amino)-methyl)-4*H*-1,2,4-triazole (L10), with one additional nitrogen donor moiety at each side of the triazole unit, appropriately disposed to yield dinuclear complex cations, $[Fe_2(L10)]^{4+}$ (**10**), similar to **6**–**9**, while coordinatively saturating both Fe centers. Such molecules are prone to exhibit SCO properties regardless of the nature of the counter-ion, which cannot act as a ligand. Unfortunately, the lack of structural information prevented the authors from extracting the coordination differences caused by solvation effects on the SCO behavior [41]. Following a commendable effort in synthetic organic chemistry, a large series of derivatives of L10 was prepared with various substituents at position four of the central tetrazole. This substituent affects the SCO, promoting either complete, gradual [LS–HS] to [HS–HS] transitions or even the persistence of the HS state in both metals. It was concluded that the differences were rather attributed to packing effects than to electronic effects [42]. One such complex, $[Fe_2(L11)](BF_4)_4$ (**11**; L11, 3,5-bis-(((2-pyridylmethyl)-amino)-methyl)-4-(*p*-tertbutylphenyl)-1,2,4-triazole, Fig. 3), was found to exhibit abrupt SCO between the [LS–HS] and the [HS–HS] states with a 22 K wide hysteresis loop [24]. A scan rate dependence of this loop showed that the experimental dynamics only affects the position of the cooling branch, making the loop wider upon decreasing the temperature scan rate. In a very interesting development with this kind of ligand, a similar family of compounds of the parent ligand 3,5-bis-(((2-pyridylmethyl)-sulfanyl)-methyl)-4*H*-1,2,4-triazole (L12) was obtained [43]. Substituent effects were investigated with this set of donors in the series $[Fe_2(L12)]^{4+}$ (**12**), featuring N_4S_2 coordination environments around the metal centers. This is of interest since Fe(II) complexes exhibiting this environment and the SCO behavior are very scarce. This unveiled a variety of SCO properties, including the observation of the [LS–LS] state in

Table 1
A list of all SCO complexes featured in this review, together with the main parameters of their magnetic behavior.

Complex	Guest/solvent	D	$T_{1/2}(\uparrow)$	$T_{1/2}(\downarrow)$		Ref
$[Fe_2(L1)_5(NCS)_4]$ (**1**)	–	0D	150	=	abr.	[27]
$[Fe_2(L2)_5(NCS)_4]$ (**2**)	–	0D	115	=	inc., gr.	[28]
$[Fe_2(L3)_5(NCS)_4]$ (**3**)	MeOH·EtOH	0D	116	=	inc., gr.	[29]
	H_2O	0D	–	–	HS	
$[Fe_2(L4)_5(NCS)_4]$ (**4**)	MeOH·EtOH	0D	116	=	inc., gr.	[30]
	EtOH	0D	122	=	inc., gr.	
$[Fe_2(L5)_5(NCS)_4]$ (**5**)	H_2O	0D	150	=	gr.	[31]
$[Fe_2(NCSe)_2(L7)_2(py)_2]$ (**6**)	–	0D	109	=	abr.	[36]
$[Fe_2(L9)_2(MeCN)_4](BF_4)_4$ (**7**)	MeCN	0D	369	356	inc., gr.	[39]
$[Fe_2(L9)_2(EtOH)_4](BF_4)_4$ (**8**)	–	0D	–	–	HS	
$[Fe_2(L9)_2(H_2O)_4](BF_4)_4$ (**9**)	–	0D	–	–	HS	
$[Fe_2(L10)](X)_4$ (**10**)	Variable	0D	Variable or undefined			[41]
$[Fe_2(L11)](BF_4)_4$ (**11**)	H_2O	0D	217	195	abr.	[24]
$[Fe_2(L12)]^{4+}$ (**12**); R=Ph	H_2O	0D	265	=	3-st.	[43]
			210	=	gr.	
			87	=		
R = tolyl	$MeCN/H_2O$	0D	109	=	inc.gr.	
R = ^{i}Bu	$MeCN/H_2O$	0D	–	–	HS	
$[Fe_2(L13)](BF_4)_4$ (**13**)	DMF	0D	280	=	inc.gr.	[44]
$[Fe_2(L14)]X_4$ (**14**); X = ClO_4^-	MeCN	0D	140[a]	=	inc.abr.	[45]
X = BF_4^-			–	–	HS	
X = $CF_3SO_3^-$			173[a]	147[a]	inc.abr.	
$[Fe_2(L15)_3](BF_4)_4$ (**15**)		0D	–	–	HS	[50]
$[Fe_2(L16)_3](BF_4)_4$ (**16**)		0D	>400	und.	gr.	[50]
$[Fe_2(L17)_3](BF_4)_4$ (**17**)		0D	–	–	LS	[51]
$[Fe_2(L18)_2](PF_6)_4$ (**18**)	$MeCN/H_2O$	0D	426	437	inc.gr.	[52]
Cl@$[Fe_2(L19)_3]Cl(PF_6)_2$ (**19**)	MeOH	0D	265	und.	inc.gr.	[54]
Br@$[Fe_2(L19)_3]Br(PF_6)_2$ (**20**)	MeOH	0D	305	und.	inc.gr.	[54]
$[Fe_2(NCS)_4(CL1)_2(L20)]$ (**21**)	MeOH	0D	105[a]	105[a]	inc.gr.	[60]
$[Fe_2(NCS)_4(CL2)_2(L20)]$ (**22**)		0D	191	=	2-st.	[61]
			218	=	gr.	
$[Fe_2(CL3)_2(L21)(ROH)_2]$ (**23**)		0D	–	–	HS	[62]
$[Fe_2(NCS)_4(CL2)_2(L22)]$ (**24**)	(polym. 1) –	0D	132	=	2-st.	[63]
			215	=	gr.	
	(polym. 2) -		–	–	HS	
	MeOH		159	=	abr.	
$[Fe_2(NCBH_3)_4(CL2)_2(L20)]$ (**25**)		0D	203	=	2-st.	[65]
			223	=	abr.	
$[Fe_2(NCBH_3)_4(CL2)_2(L21)]$ (**26**)		0D	290	=	gr.	[65]
$[Fe_2(NCBH_3)_4(CL2)_2(L23)]$ (**27**)		0D	241	=	gr.	[65]
$[Fe_2(L24)_2(NCS)_4]\cdot$(**28**)	$4CH_2Cl_2$	0D	180	=	2-st.	[66]
			80	=	gr.	
	CH_2Cl_2		200	=	gr.	
$[Fe_2(L25)(H_2O)_2(MeOH)_2](ClO_4)_2$ (**29**)	MeOH	0D	–	–	HS	[68]
$[Fe_2(L25)(H_2O)_2(MeCN)_2](BF_4)_2$ (**30**)	MeCN	0D	265	=	inc.gr.	[68]
$[Fe_2(L25)Cl_2](CF_3SO_3)_2$ (**31**)	Benzylcyanide	0D	–	–	HS	[68]
$[Fe_2(L26)_2(NCS)_2]$ (**32**)	DMF/H_2O	0D	125	und.	inc.gr.	[69]
	–		184	189	abr.	
$[Fe_2(L27)_2(NCS)_2]$ (**33**)	DMF/H_2O	0D	210	=	2-st.	[69]
			130	=	gr.	
$[Fe_2(SCN)_4(L28)_2]$ (**34**)	H_2O	0D	–	–	HS	[70]
$[Fe_2(L29)_2(CL4)_2]$ (**35**)	–	0D	350[a]	=	gr.	[71]
$[Fe_2(L29)_2(CL5)_2]$ (**36**)	MeOH	0D	180	=	gr.	[71]
	–		196	=	gr.	
$[Fe_2(L30)(CL4)_2](TFPB)_2$ (**37**) F-sub	THF/hexane	0D	160	=	gr.	[72]
Cl-sub			124	=	gr.	
Br-sub			121	=	gr.	
H-sub			110	=	gr.	
$[Fe_2(L31)(CL4)_2](OTf)_2$ (**38**)	CH_2Cl_2	0D	195	=	2-st.	[73]
			235	230	inc.gr.	
$[Fe_2(L32)(CL4)_2](OTf)_2$ (**39**)	CH_2Cl_2/MeCN	0D	285[a]	230[a]	inc.gr.	[73]
$[Fe_3(L33)_6(H_2O)_6]$ (**40**)	H_2O phase 1	0D	150	=	inc.gr.	[77]
	H_2O phase 2		357	343	inc.abr.	
	–		–	–	HS	
$(Me_2NH_2)_6[Fe_3(L34)_6(H_2O)_6]$ (**41**)	H_2O	0D	>400	310	inc.gr.	[78]
$[Fe_3(L35')_2(L35)_2](BF_4)_2$ (**42**)	MeCN	0D	–	–	LS/HS/LS	[74]
	–		355	329	inc.abr.	

Table 1 (*continued*)

Complex	Guest/solvent	D	$T_{1/2}(\uparrow)$	$T_{1/2}(\downarrow)$		Ref
$[Fe(L37)_3](R\text{-}CSA)_2$ (**43**)	–	1D	316	300	gr.	[97]
R-CSA = camphorsulfonate	2-BuOH(rac)		324	315	abr.	
	R-2-BuOH		325	316	abr.	
	S-2-BuOH		323	314	abr.	
$[Fe(L38)_3](DBS)_2$ (**44**)	–	1D	318	306	gr.	[98]
DBS = 4-dodecylbenzenesulfonate						
$[Fe(L39)_3](BF_4)_2$ (**45**)	–	1D	188	172	abr.	[99]
			235	230	2-st.	
$[Fe(L40)_3](X)_2$ (**46**) X = ClO_4^-	–	1D	296	291	abr.	[100]
	CH_3OH		273	263		
X = NO_3^-	–		338	278		
	H_2O		353	333		
X = BF_4^-	–		106	92		
	H_2O		320	305		
X = $CF_3SO_3^-$	H_2O		325	322		
$[Fe(L41)_3]I_2$ (**47**)	H_2O	1D	292	275	abr.	[101]
$[Fe(L42)Pt(CN)_4]$ (**48**)	–	3D	309	285	abr.	[109]
	Maleic anhydride		209	200	2-st.	
			186	170	abr.	
	Maleic acid		159	155	inc.	
$[Fe(L43)(Au(CN)_2)_2]$ (**49**)	EtOH	3D	203[a]	200[a]	4-st.	[113]
			178[a]	172[a]		
			145[a]	125[a]		
			107[a]	85[a]		
$[Fe(L44)Pt(CN)_4]$ (**50**)	EtOH	3D	154	138	3-st.	[116]
			148	127		
			134	115		
$[Fe(L42)(Au(CN)_2)_2]$ (**51**)	–	3D	367	349	abr.	[117]
$[Fe(L45)_2(Au(CN)_2)_2]$ (**53**)	–	3D	148	=	gr.	[120]
	DMF/EtOH/cyclochexane		153	143	2-st.	
			134	126	gr.	
	Cyclochexane		129	123	inc.	
	BuOH		209	186	2-st.	
			189	171		
	i-BuOH		222	217	2-st.	
			211	205		
	EtOH		251	249	2-st.	
			226	208		
$[Fe(L46)(Au(CN)_2)_2]$ (**54**)	–	3D	204	=	2-st.	[121]
			134	=		
$[Fe(L46)(Ag(CN)_2)_2]$ (**55**)	–	3D	232	=	2-st.	[121]
			216	=		
$[Fe(L23)Pt(CN)_4]$ (**56**)	L23	3D	240	=	3-st.	[124]
	H_2O		216	212		
			200	197		
	L23		210	=		
			181	178		
			164	160		
	1,2-dibenzylethane		160[a]	=	gr.	
	Stilbene		163	=	abr.	
$[Fe(L47)(Au(CN)_2)_2]$ (**57**)	DMF,EtOH,C_6H_{12}	3D	175	=	gr.	[125]
	C_6H_{12}		142	136	inc.	
	C_6H_6		221	207	3-st.	
			155	155		
			144	139		
	CS_2		190	167	abr.	
	Naphthalene		214	141	abr. inc.	
	Ferrocene		166	129	gr. inc.	
	Anthracene		151	131	gr. inc.	
	–		156	156	2-st.	
			119	110		
$[Fe(L20)(Au(CN)_2)_2]$ (**58**)	Benzene	3D	233	222	abr.	[126]
	Toluene		234	231		
	o-xylene		220	217	3-st.	
			184	176		
			136	132		
	m-xylene		234	232	2-st.	
			208	206		
	p-xylene		266	246	3-st.	
			214	212		
			185	182		
	Chloroform		184	128	inc.	

(*continued on next page*)

Table 1 (*continued*)

Complex	Guest/solvent	D	$T_{1/2}(\uparrow)$	$T_{1/2}(\downarrow)$		Ref
$[Fe(L20)Ni(CN)_4]$ (**59**)	H_2O	3D	–	–	HS	[127]
	EtOH		223	213	2-st.	
			197	187		
	Acetone		145	125	abr.	
$[Fe(L48)_{2/3}(M(CN)_2)_2]$ (**60**); M = Ag	CH_2Cl_2	3D	244	=	gr.	[129]
	Furan		209	=		
	Pyrrole		167	=		
	Thiophene		152	=		
M = Au	CH_2Cl_2		222	=		
	Furan		199	=		
	Pyrrole		197	=		
	Thizophene		137	=		
$[Fe(L50)(Au(CN)_2)_2]$ (**65**)		3D	263	221	abr.	[132]
$[Fe(CL7)_2M(CN)_4]$ (**66**); M = Ni		2D	198	190	2-st.	[135]
			182	173	abr.	
M = Pd			215	205	2-st.	
			150	145	gr.	
M = Pt			115	101	abr.	
$[Fe(CL10)_2(Au(CN)_2)_2]$ (**67**)		2D	222[a]	218[a]	abr.	[137]
$[Fe(CL11)_2(Au(CN)_2)_2]$ (**68**)	CL11	2D	250	250	2-st.	[138]
		2D	93	92		
	–		124	=	gr.	
$[Fe(L3)_2Pt(CN)_4]$ (**69**)	–	2D	154	152	inc.	[139]
$[Fe(CL12)_2Pd(CN)_4]\cdot nH_2O$ (**70**)	–	2D	204	184	abr.	[140]
$[Fe(CL13)_2M(CN)_4]$ (**71**); M = Pd	–	1D	272	270	gr.	[141]
M = Pt	–		274	272		
$[Fe(CL14)_2M(CN)_4]$ (**72**); M = Pd	–	1D	186	=	abr.	
M = Pt			184	=		
$[Fe(CL15)_2M(CN)_4]$ (**73**)	–	1D	350[a]	=	gr.	[142,143]
					inc.	
$[Fe_2(CL16)_8Nb(CN)_8]$ (**74**)	–	3D	130	=	gr.	[144]
$[Fe_2(CL18)_8W(CN)_8]\cdot nH_2O$ (**76**)	H_2O	3D	200	=	gr.	[146]
$[Fe(L51)_3](ClO_4)_2$ (**77**)	–	1D	204	200	gr.	[147]
	CO_2		212	209		
$[Fe(L53)_3]X_2$ (**79**) X = ClO_4^-	–	1D	150	149	abr.	[149]
X = BF_4^-			161	158		
$[Fe(L54)_3](ClO_4)_2$ (**80**)	MeCN	1D	165	165	2-st.	[150]
			96	90		
$[Fe(L55)]$ (**81**)		2D	226	218	abr.	[151]
$[Fe(L56)_2]$ (**82**)	–	2D	192	=	2-st.	[153]
			144			
	MeOH		176	173		
			128	127		
	EtOH		158	154		
			121	113		
$Fe(L57)_3]X_2$ (**83**) X = ClO_4^-	H_2O	3D	265	=	abr.	[154]
	–		285	=		
X = BF_4^-	H_2O		284	=		
	–		290	=		
$[Fe(L58)_2]$ (**84**)			501	=	2-st.	[155,156]
			329		gr.	
$[Fe(L59)_2]$ (**85**)			419	=	gr.	[155,156]
$[Fe(L60)_2]$ (**86**)			416	=	gr.	[155,156]
$[Fe(L61)_2(NCX)_2]$ (**87**)	MeCN	2D	129	=	2-st.	[157]
			78			
	Acetone		90[a]	–	inc.	
$[Fe(L47)_2(NCX)_2]$ (**88**); NCS^-	$EtOH/H_2O$	3D	–	–	HS	[158]
	EtOH	2D	–	–	HS	
$NCSe^-$	$EtOH/H_2O$	3D	82	=	inc.	
	CH_2Cl_2	3D	96	=		
	$EtOH/H_2O$					
$[Fe(L47)_2(NCBH_3)_2]$ (**89**)	$EtOH/H_2O$	2D	247	=	abr.	[158]
	$EtOH/CL_2CH_2$		189	=	abr.	
$[Fe(L20)_2(H_2O)_2](ClO_4)_2$ (**90**)	L20	2D	200[a]	=	gr.	[159]
	H_2O					

Table 1 (*continued*)

Complex	Guest/solvent	D	$T_{1/2}(\uparrow)$	$T_{1/2}(\downarrow)$		Ref
$[Fe(L22)_2(SCN)_2]\cdot S$ (**91**)	PhCHO	2D	194	194	2-st.	[160]
S = various guests			176	168	gr.	
	MeCN,H_2O	223		=	2-st.	
		204			gr.	
	DMSO,H_2O	195		=	2-st.	
		163			gr.	
	DMA,H_2O	187		=	2-st.	
		145			gr.	
	L22,H_2O	221		=	2-st.	
		204		201	gr.	
	PhCN		224	224	2-st.	
			202	198	gr.	
	$PhNO_2$		226	226	2-st.	
			197	191	gr.	
	–		–	–	HS	
$[(Fe(NCS)_2)_3(L62)_4]$ (**92**)	CH_2Cl_2 EtOH	3D	152	142	gr.	[164]
$[Fe(L63)(NCS)_2]$ (**93**)	MeOH	1D	≈300	=	inc.	[165]
	–		358	=	2-st.	
			172		gr.	
$[Fe(CL19)(L64)](BPh_4)_2$ (**94**)	Acetone	1D	–	–	HS	[166]
	–		212	=	gr.	
[Fe(CL3)(L21)] (**95**)	EtOH	1D	190	170	2-st.	[62]
			135	110	abr.	
	DMF		305	=	gr.	
	Toluene		125	=	gr.	
	(annealed)	?	320	=	3-st.	
			210		gr.	
			140			
[Fe(CL3)(L65)] (**96**)		1D	105	90	inc.	[167]
$[Fe(L66)(L67)](ClO_4)$ (**97**)		2D	146	=	inc.	[168]

[a] Estimated from the graphic plot. $T_{1/2}(\uparrow)$ and $T_{1/2}(\downarrow)$ are the temperatures (in K) of the thermal spin crossover upon warming and cooling, respectively, defined as the temperature where 50% of the conversion occurs with respect to the total number of centers that experience the transition.

some of the derivatives, and also revealed that the tendencies observed in the solid state are opposite to those seen in solution. Thus, the SCO in the solid state is dominated by packing effects whereas the σ-donating ability of the triazole substituent dominates the SCO temperature in solution. Another variation in this category of ligands is changing the nature of the central heterocycle. Thus, ligand 2,5-bis-((2-pyridylmethyl)-amino)-methyl-1,3,4-thiadiazole (L13) combines the bridging N–N diazole in this ring with an atom of sulfur [43]. This leads undoubtedly to changes in the electronic environment around the metal centers and, according to the authors, also provides a higher flexibility in the coordination geometry. As a result, the corresponding $[Fe_2(L13)]^{4+}$ (**13**) cations have a marked tendency to remain in the [LS–LS] state, only starting to undergo thermal SCO above 250 K. This family was used to illustrate the crucial influence of the lattice solvent molecules on their solid-state magnetic properties [44]. Thus, while the complex **13**$(BF_4)_4\cdot$4DMF is in the [LS–LS] state up to 300 K, the desolvated product becomes [HS–HS] near room temperature with the spin transition to the [LS–HS] state occurring at 280 K. This transformation can be reversed to yield **13**$(BF_4)_4\cdot$4DMF by exposing the solid to a DMF atmosphere.

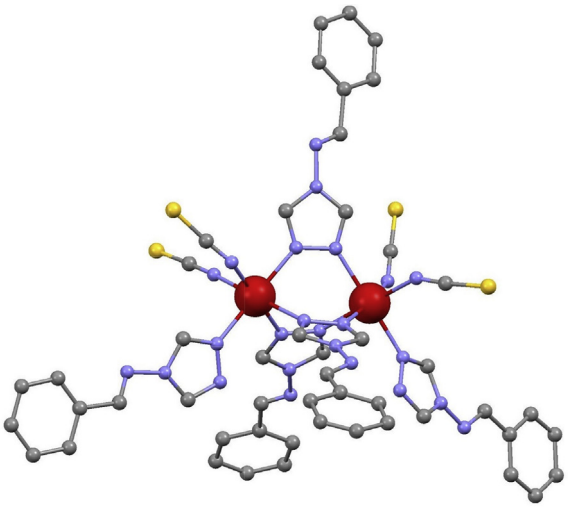

Fig. 2. Molecular structure of $[Fe_2(L2)_5(NCS)_4]$ (**2**) [28]. Color guide: Fe (LS), red; C, grey; N, purple; S, yellow. H-atoms are not shown.

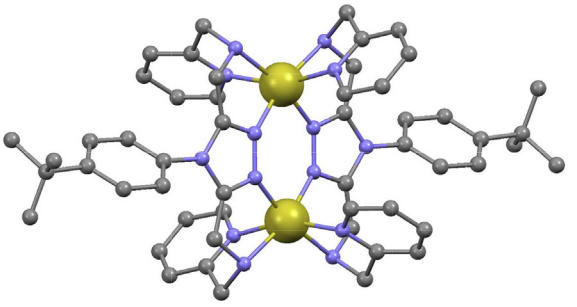

Fig. 3. Molecular structure of $[Fe_2(L11)](BF_4)_4$ (**11**) [24]. Color guide: Fe (HS), yellow; C, grey; N, purple. H-atoms are not shown.

This desorption/adsorption process is robust and can be repeated for several cycles, with the consequent changes in the magnetic properties.

In view of these interesting results, this research was extended to the ligand 2,5-bis-((2-pyridylmethyl)-amino)-methyl-1,3,4-oxadiazole (L14), with an oxygen atom substituting the sulfur atom in the central diazole ring [45]. The set of compounds $[Fe_2(L14)]X_4$ (**14**) exhibits SCO features, with a high dependency on the counter anion, ranging from [HS–HS] in the whole temperature range studied ($X = BF_4^-$) to a [HS–HS] to [LS–HS] transition around 147 K ($X = ClO_4^-$), sometimes with a 26 K wide hysteresis. This is a very rare case of hysteresis of a polynuclear SCO complex.

2.1.2. Triple stranded helicates or mesocates

Very few coordination supramolecular helicates [46,47], have been exploited in the context of SCO. Here, helicates are coordination complexes of two or more metals contained in the axis of a helix, coordinated by bridging ligands that constitute the strands. In the case of dinuclear systems, if the metal centers possess opposite chirality, the molecules are mesocates (they are identical to their mirror image) instead of helicates. Among the earliest precedents is a family of Fe(II) dinuclear triple-stranded helicates made of bis-methyleneimineimidazole moieties. These helicates exhibit spin transitions around room temperature, of varying degrees of completeness and temperatures $T_{1/2}$, depending on the nature of the counter-ion (i.e. PF_6^-, BF_4^- or ClO_4^-) [48]. A related helicate with a very similar ligand showed solvent-dependent magnetic properties and a very rich photomagnetic behavior [49]. Much more recently, an analogous ligand, comprising a shorter spacer (*N*,*N*′-bis(1*H*-imidazol-4-ylmethylene)benzene-1,3-diamine, L15), was shown to impose a strain within the molecular ensemble, causing the formation of a *mesocate* ($[Fe_2(L15)_3](BF_4)_4$, **15**) rather than a helicate, with fixed Fe–N distances that stabilize the [HS–HS] state down to 2 K [50]. The equivalent to L15 with pyridyl, rather than imidazolyl (*N*,*N*′-bis(pyridine-2-ylmethylene) benzene-1,3-diamine, L16) causes the same effects, producing the corresponding mesocate $[Fe_2(L16)_3](BF_4)_4$ (**16**). But in this case, a spin transition occurs at 350 K. This is in contrast to what is expected for pyridylimine Fe(II) tris-chelates, usually found in the LS state. A similar ligand featuring two connected 1-(2-pyridyl)pyrazoles instead of imidazolimines (4,4′-(methylene)-bis-(1-(2-pyridyl)pyrazole, L17) also yields the expected helicate, $[Fe_2(L17)_3](BF_4)_4$ (**17**) [51]. This complex was characterized by SCXRD and also in solution, via ^1H NMR and mass spectrometry (MS). All these experiments confirmed the [LS–LS] ground state, and no appearance of SCO behavior.

The ligand 1,1′-(1,2-ethanediyl)-bis-1,2,3-triazol-4-yl-methylideneamino-2-ethylpyridine (L18) comprises two tridentate '*N*,*N*,*N*' coordination pockets separated by a flexible spacer [52]. This provides this donor with the ability to form double stranded (instead of triple stranded) dinuclear helicates around six-coordinate metal ions. The complex formed by the reaction of L18 with $Fe(PF_6)_2$, $[Fe_2(L18)_2](PF_6)_4$ (**18**), falls under this definition.

It shows a multistep SCO, with a first gradual transition reaching an about 50% [HS–HS] state and then an abrupt transition reaching completeness. The abrupt regime shows an 11 K wide hysteresis. No other helicates featuring hysteresis have been reported so far.

SCO supramolecular helicates can potentially encapsulate functional guests as a way to combine magnetic switching abilities with a second property. This shall be done using the central cavity in the assembly. Benefiting from its internal symmetry and its ability to establish supramolecular interactions with guests, ligand 1,3-bis[1-(pyridine-2-yl)-pyrazol-3-yl]benzene (L19) exhibits two pyrazolyl pyridine chelating units, known to provide SCO properties to Fe(II) [53] and separated by a phenylene spacer [54]. The N–H moieties of the pyrazolyl fragments point towards the interior of the helicate formed upon coordination with Fe(II), thus becoming poised for their interaction through hydrogen bonds with guests acting as acceptors. This cavity is well suited for fixing Cl^- or Br^- anions. Thus, the composite supramolecular ensembles $X@[Fe_2(L19)_3]X(PF_6)_2$ (X = Cl, **19**; Br, **20**, Fig. 4) were prepared and characterized. SCXRD and magnetic measurements showed that **19** and **20** exhibit ordered [LS–HS] mixed-spin states that can be brought thermally to the [HS–HS] state. The SCO temperature of the guest molecules is shifted by 40 K on going from Br^- to Cl^- (from 265 to 305 K). The SCO can be followed by monitoring the average Fe–N distances with temperature (Fig. 4). Interestingly, **19** and **20** experience SCSC transformations upon exposure to air, by exchange of some lattice MeOH molecules by H_2O. The resulting solvatomorphs experience a two-step (**19**, Cl) or a gradual (**20**, Br) SCO from the [HS–HS] to the [LS–LS] on passing through the [LS–HS] species. The three states of these hydrates were also characterized by SCXRD. ^1H NMR and MS demonstrated the persistence of these inclusion helicates in solution, together with small amounts of the guest free species, as well as of a supramolecular assembly resulting from the recognition of two mononuclear $[Fe(L19)_3]^{2+}$ units entangled together with a central X^- (Cl or Br) anion. The latter could be subsequently isolated under appropriate experimental conditions and characterized [55].

2.1.3. Complexes with 4,4′-dipyridyl-type ligands

A useful approach to prepare multinuclear SCO compounds consists of linking preformed coordinatively unsaturated coordination complexes with the appropriate bridging ligands. Complexes possessing labile, easy to substitute ligands are also suitable building blocks. Poly-pyridyl ligands are perhaps the most popular bridging ligands in this area of supramolecular coordination chemistry [56–59]. In the context of Fe(II) SCO, the first dinuclear complexes made in this way were based on the bridging ligand 4,4′-bipyridine (L20) [60]. Complex $[Fe_2(NCS)_4(CL1)_2(L20)]$ (**21**; CL1, 2,6-bis-(3-pyrazolyl)-pyridine, as seen in Fig. 5), features two equivalent, separated Fe(II) building blocks within a molecule, each containing two *trans*-NCS^- terminal ligands in addition to a *meridional* (*mer*) capping ligand (CL1). The ensemble exhibits a [LS–HS] to [HS–HS] transition triggered thermally or by light irradiation through the light induced excited spin state trapping (LIESST) effect at low temperatures. Changing the capping ligand from CL1 to di(2-picolyl)amine (CL2) leads to the analogous complex $[Fe_2(NCS)_4(CL2)_2(L20)]$ (**22**) [61]. Since the capping ligand is

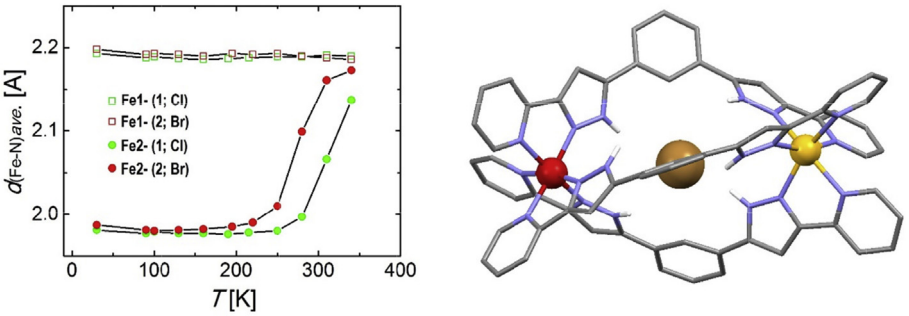

Fig. 4. (left) Temperature dependence of the average Fe–N distances for compounds X@[$Fe_2(L19)_3$]Br(PF_6)$_2$ (**19** and **20**) as determined through single crystal X-ray diffraction and (right) molecular structure of **20** [54]. Color guide: Fe (LS), red; Fe (HS), yellow; C, grey; N, purple; H, white. Only H-atoms of N-H groups are shown.

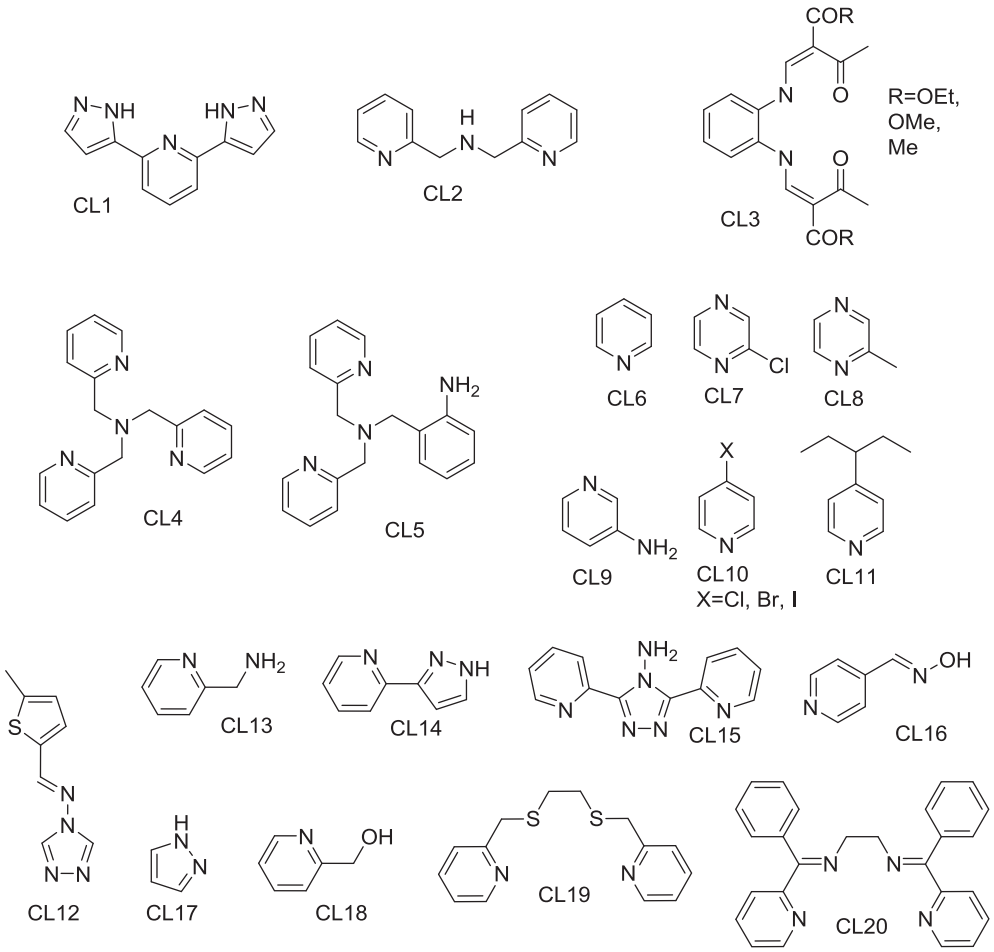

Fig. 5. Structure of capping ligands mentioned in this review.

now *facial* (*fac*), the NCS^- ligands in **22** are *cis*. This complex exhibits a two-step transition from [LS–LS] to [LS–HS], and then to [HS–HS]. The related bridging ligand 4,4′-dipyridylethyne (L21) was employed in combination with the N_2O_2 Schiff base donor CL3. Since the latter occupies the four equatorial positions around a metal center in a square geometry, it leaves only the two remaining octahedral sites in *trans* conformation. This favors, in combination with linear bridging ligands, the formation of 1D coordination polymers (see below). Discrete dinuclear complexes can also be obtained capping both ends with solvent or other terminal ligands, leading for example to [$Fe_2(CL3)_2(L21)(ROH)_2$] (**23**, R = Me or Et) [62]. The nature of the donor atoms around the Fe(II) centers, N_3O_3, favors an HS state,

which is observed at all temperatures. Metathesis of these alcohols by terminal N-ligands could provide SCO properties to these assemblies.

Subsequent synthetic work was conducted to draw structural/property correlations by changing the bridging ligand while maintaining the molecular structure intact in the series $[Fe_2(NCS)_4(CL2)_2(L)]$ (e.g., L = L20, **22**; L22, 4,4′-dipyridylethene, **24**). These studies revealed that simply comparing solvatomorphs or even polymorphs of the same compound yields completely different magnetic properties [63]. Analysis of the magnetic properties of **22** and **24**, for example, revealed that the SCO properties were mostly related to the local distortion around the FeN_6 coordination polyhedron, rather than to the electronic or structural properties of the bridging ligands [64]. These distortions are in turn related to the packing of the molecules within the crystal lattice. This study was completed with the synthesis of a new family of compounds, this time featuring a new terminal ligand: $NCBH_3^-$. The new group of compounds, $[Fe_2(NCBH_3)_4(CL2)_2(L)]$ (L = L20, **25**; L21, **26**; L23, 4,4′-dipyridylethane, **27**), elegantly confirmed the conclusions extracted from the previous investigation [65].

2.1.4. Complexes with poly-dipyridyl-type ligands

The evidence that pyridyl donor groups favor the manifestation of SCO properties upon coordination to Fe(II) centers has motivated the synthesis of ligands incorporating several such groups. Some of these were designed as bridging ligands, following the work with the bis-pyridine species of the previous section. Complex $[Fe_2(L24)_2(NCS)_4]$ (**28**; L24, 2,5-bis-(2′,2″-dipyridylamino)pyridine) was a remarkable contribution since it exhibits a two-step SCO between the [LS–LS] ground state, the intermediate [LS–HS] and the [HS–HS]. The crystalline stability through these transitions allowed, for the first time in a dinuclear system, complete SCXRD characterization for the three states [66]. This compound, prepared as a solvate with four CH_2Cl_2 molecules per unit, exhibits remarkable partial or total desolvation effects, which are reversible and are accompanied by drastic changes in the magnetic properties. The dependence of these properties as a function of solvation with CH_2Cl_2 or $CHCl_3$, as well as their capacity to undergo the LIESST effect, were reported in a subsequent paper [67].

A related ligand comprising three chelating units, 2,4,6-tris-(2′,2″-dipyridylamino)-1,3,5-triazine (L25), also yields dinuclear Fe(II) complexes [68]. The complexes $[Fe_2(L25)(H_2O)_2S_2]X_2$ (S, X = MeOH, ClO_4^-, **29**; MeCN, BF_4^-, **30**) exhibited strong solvent-dependent magnetic properties, from an SCO system (**29**) to a fully HS complex at all temperatures (**30**). The related complex $[Fe_2(L25)Cl_2](CF_3SO_3)_2$ (**31**) is in the [HS–HS] state down to low temperature, where the onset of very unusual ferromagnetic coupling between Fe(II) centers is detected.

More recently, two new polypyridyl ligands have been reported: 2,5-bis-(*N*,*N*-bis-(2-pyridylmethyl)aminomethyl)-pyrazine (L26) and 2,3-bis-(*N*,*N*-bis-(2-pyridylmethyl)aminomethyl)-pyrazine (L27) [69]. These ligands possess up to eight N-donor atoms, and they react with Fe(II) to form dinuclear complexes engaging all nitrogen atoms, thus acting as bis-tetradentate ligands. The resulting complexes, $[Fe_2(L26)_2(NCS)_2]$ (**32**) and $[Fe_2(L27)_2(NCS)_2]$ (**33**), show very gradual SCO to the [HS–HS] state, starting from an intermediate [LS–HS] state and from a quasi-pure [LS–LS] state, respectively. Upon desolvation at 400 K (by loss of one molecule of DMF and two molecules of H_2O), complex **32** (desolvated) exhibits an extremely abrupt transition with a small hysteresis ($T_{1/2}$ values of 184 and 189 K). Desolvated **32** and complex **33** showed a rapid transition to metastable [HS–HS] states when irradiated at low temperature with green light (532 nm). In both cases, this transition unveiled the existence of intramolecular antiferromagnetic interactions.

Three ligands related to L26 and L27 were prepared in order to further extend this investigation. These are close to L28 (4,6-bis-(*N*,*N*-bis-(2-pyridylmethyl)aminomethyl]-2-phenylpyrimidine), but comprising a central pyrimidine (instead of pyrazine) [70], with half or all of the methylpyridine arms replaced by ethylpyridine. In all cases, complexes analogous to $[Fe_2(SCN)_4(L28)_2]$ (**34**) were obtained. Furthermore, the NCS^- ligand could also be replaced by $NCSe^-$ or $NCBH_3^-$. Interestingly, unlike with the previous examples, all these compounds were found in the [HS–HS] state at all temperatures. The authors of this study suggest that the weaker field furnished by the pyrimidine central ring is the reason for this magnetic behavior. They also mentioned strongly distorted coordination for the metal centers, which could favor the [HS–HS] spin state observed in this family of compounds.

2.1.5. Complexes with other types of bridging ligands

A few other bridging ligands have been used recently to form dinuclear Fe(II) molecules with SCO properties. One interesting ligand is the cyanocarbanion L29 (2-dicyanomethylene-1,1,3,3-tetracyanopropanediide dianion) [71]. The use of flexible tetradentate capping ligands CL4 (tris(2-pyridylmethyl)amine) and CL5 (bis(2-pyridylmethyl)-(2-anilylmethyl)amine) leaves two remaining sites on Fe(II), featuring a *cis* configuration, in perfect disposition for the binding of two L29 ligands and the formation of dinuclear complexes $[Fe_2(L29)_2(CL4)_2]$ (**35**) and $[Fe_2(L29)_2(CL5)_2]$ (**36**). Both complexes exhibit SCO, at very different transition temperatures (more than 170 K difference). It is worthy to mention that compound **35** is obtained as a MeOH solvate (one methanol molecule per complex), but it is immediately desolvated on contact with air. Therefore, the magnetic data available correspond to the desolvated compound. On the other hand, **36** is prone to solvent desorption during the magnetic measurements, making the initial cooling and warming branch not superimposable. In any case, the desolvate shows the transition near room temperature.

The ligand 2,5-dianilino-1,4-benzoquinone (L30) was prepared with various substituents 'X' at positions '3' and '6' (X = H, F, Cl, Br, I) in order to study the electronic effects on the SCO properties of the dinuclear complexes $[Fe_2(L30)(CL4)_2](TFPB)_2$ (**37**) and the derivatives, prepared by design, using CL4 as the capping ligand (TFPB = tetrakis-(3,5-bis(trifluoromethyl)phenyl)borate) [72]. The five derivatives experience a one-step incomplete SCO from a mixture of [LS–HS]/[HS–HS] states to the [HS–HS] state. $T_{1/2}$ correlates with the substituent in the order H > Br > Cl > F. The percentage of HS Fe centers remaining at low temperature follows the inverse order, consistent with larger stabilization of the HS by a more

electronegative substituent. If the temperature is decreased further, magnetization data indicate the existence of ferromagnetic interactions between HS Fe(II) centers.

The quantified magnetic susceptibility data confirmed that the mixed ground spin state is formed by [LS–HS] and residual [HS–HS] with no population of the [LS–LS] state. The latter was corroborated by Mössbauer spectroscopy, which probed the exclusive presence of these two conformations.

Symmetric L31 (double deprotonated 2,5-bis-(4-(isopropyl)anilino)-1,4-benzoquinone) and asymmetric L32 (double deprotonated 2-(4-(isopropyl)anilino)-5hydroxy-1,4-benzoquinone) are two quinoid derivatives of L30. The corresponding dinuclear complexes $[Fe_2(L31)(Cl4)_2](OTf)_2$ (**38**) and $[Fe_2(L32)(Cl4)_2](OTf)_2$ (**39**) were prepared in order to compare a symmetric complex with an asymmetric one [73]. Complex **38** behaves in a similar way to **37** and its analogues (see above), exhibiting an incomplete SCO, structured in two steps (one more gradual than the other) at higher $T_{1/2}$. At low temperature, evidence of ferromagnetic coupling within the [HS–HS] species was also observed. The authors propose that the low temperature regime contains a mixture of [LS–LS], [LS–HS] and [HS–HS] species, following two subsequent and incomplete SCO processes from [HS–HS] to [LS–HS], and then from the latter to [LS–LS]. The asymmetric analogue (**39**) exhibits a much cleaner SCO from a mixed spin system (probably [LS–HS]) to a [HS–HS] with a wide hysteresis. The low temperature regime does not indicate any kind of exchange coupling, suggesting that the system is composed exclusively of the [LS–HS] species.

2.2. Trinuclear complexes

Most of the trinuclear Fe(II) complexes exhibiting spin transition are linear species of three metal ions linked pairwise by triple bridges made of 1,2,4-triazoles. The early examples consist of three Fe(II) in the HS state, of which the central one, with an FeN_6 coordination environment, undergoes a spin transition to the LS state upon cooling [74–76]. These molecules always respond to the general formula $[Fe_3(trz)_6(L)_6](A)_6$, where trz is a triazole ligand, L is a neutral monodentate ligand (usually solvent molecules) and A^- is a counterion. Very recently, an interesting variation of this pattern was reported, using a 1,2,4-triazole bridging ligand bearing a negatively charged substituent: 4-(1,2,4-triazol-4-yl)ethanesulfonate (L33) [77]. The reaction of an organic salt of L33 with $Fe(ClO_4)_2$ in water led to $[Fe_3(L33)_6(H_2O)_6]$ (**40**), the first neutral cluster of its kind. This compound crystallizes with several molecules of water. It features three HS Fe(II) ions at room temperature. Above room temperature, **40** partially stabilizes a new [HS–LS–HS] phase with a transition to the [HS–HS–HS] state above 350 K. This SCO features a wide hysteresis in a remarkable case of high temperature cooperativity for a discrete compound ($T_{1/2}\uparrow$ = 357 K and $T_{1/2}\downarrow$ = 343 K). Interestingly, the system can be further desolvated above 370 K resulting in a [HS–HS–HS] phase at all temperatures. The three phases and their transitions following desolvation were characterized by powder X-ray diffraction. A remarkable extension of this strategy was made with the use of dianionic triazole 4-(1,2,4-triazol-4-yl) ethanedisulfonate (L34) as the bridging ligand. The resulting trinuclear complex with Fe(II) is then anionic, needing cations to achieve electroneutrality in the salt $(Me_2NH_2)_6[Fe_3(L34)_6(H_2O)_6]$ (**41**) [78]. At room temperature and below, compound **41** is found in the familiar [HS–LS–HS] state. Above 400 K, it converts into another phase that exhibits the [HS–HS–HS] state. This phase shows remarkable properties, featuring a reversible [HS–HS–HS] to [HS–LS–HS] SCO associated with a wide hysteresis ($T_{1/2}\downarrow$ = 310 K, when cooling down at an almost static scan rate). The [HS–HS–HS] state is easily trapped thermally by fast cooling, and this metastable stable state only relaxes back to the ground [HS–LS–HS] state above T_{TIESST} = 250 K, the highest observed to date.

An interesting triangular $[Fe(II)_3]$ cluster was recently obtained with the compartmental ligand L35 (3,5-bis-(6-(pyridine-2-yl)-pyridine-2-yl)-pyrazole), which was originally designed to bind two octahedral metal ions occupying three *mer* coordination positions, leading to tetranuclear $[M_4(L35)_4]^{n+}$ grid assemblies. Some of them have shown multistep SCO processes, following the sequential transition of some of their individual metal centers [79]. By reducing the amount of $Fe(BF_4)_2$ during synthesis, a defect grid $[Fe_3(L35')_2(L35)_2](BF_4)_2$ (L35′, deprotonated L35; **42**) was obtained [80]. This compound crystallizes from MeCN with two solvent lattice molecules and exhibits the [LS–HS–LS] state between 2 and 380 K (in a closed container). SCXRD data confirmed that the central Fe(II) center was in the HS state. If complex **42** desolvated by heating in an open container, the resulting system showed a [LS–HS–LS] to [LS–HS–HS] SCO with hysteresis ($T_{1/2}\uparrow$ = 355 K and $T_{1/2}\downarrow$ = 329 K). This hysteresis showed consecutive widening with repeated cycling that was associated with the gradual reduction of crystal sizes. Desolvated **42** was also shown to be sensitive to the vapors of small molecules, which in all cases drastically reduce or quench the SCO altogether.

2.3. Coordination polymers

SCO coordination polymers are built from polydentate ligands able to act as bridges between the active metal centers, thus creating a true infinite coordination structure in addition to furnishing the appropriate ligand field strength to observe this phenomenon. Only a few multidentate ligands can match these two requirements. In most cases, combinations of ligand types are necessary, including ancillary terminal ligands, to achieve all these conditions. The coordination modes, local geometry and ligand skeleton will modulate the network dimensionality.

In this section, we have classified different materials based on their bridging ligands, in order to further understand their key features and effect upon the magnetic bistability. A very comprehensive and detailed review on SCO coordination polymers was published in 2013 by Muñoz, Real et al. [15] Because of this, we will focus on the most recent 2013–2017 literature to cover the significant advances and outline some future trends in the field.

It is easy to conclude that coordination polymers are more prone to exhibit high cooperativity SCO, given the long-range connectivity between active centers as

mediated by the bridging ligands. In general, this should yield abrupt transitions and wide hysteresis, and the search for these two features was the initial driving force for their study. This is however not always the case, and many polymeric structures also exhibit non-cooperative transitions, including incomplete or multi-step transitions with intermediate phases. As discussed in the introduction, the latter is also an attractive possibility with unique technological applications.

The polymeric nature of these materials also gives them special stability in the solid state, allowing easier reversible incorporation of guest molecules into their structure when compared with discrete molecules. Post-synthetic exchange of solvents, or organic molecules, in addition to chemical reactions within their robust architecture offer unparalleled possibilities in the field, since molecular SCO materials are prone to irreversible changes upon desolvation or solid-state solvent exchange reactions. A comprehensive review on guest chemistry of SCO coordination polymers was recently published by Cirera [81].

2.3.1. Polymers with 1,2,4-triazole ligands

1,2,4-triazole (L36) and its derivatives have been exploited for decades as a source of high temperature, wide thermal hysteresis SCO materials [82–84]. Easy preparation from readily available raw materials in combination with their robust and abrupt thermal transitions at/above room temperature make them unique candidates for memory devices and sensors. The materials of this family are made using triply bridged Fe 1D chains, where all Fe centers are structurally identical, possessing an N_6 coordination environment (Fig. 6) [16,85–87]. The bistability and magnetic features of these materials, despite their stiff architecture, may be tuned by modification of the triazole functional group on the N4 position, with anions compensating the overall cationic charge (the ligands are typically neutral), and filling the open holes with the solvent in the structure. Variations of all these elements have been heavily investigated during the last few decades, and little surprises are expected. Currently, most efforts are directed to the exploitation of these materials at the nanoscale [85,88,89]. Remarkably, these SCO materials retain the memory effect down to very small sizes (<5 nm) [90,91], including core/shell architectures [92].

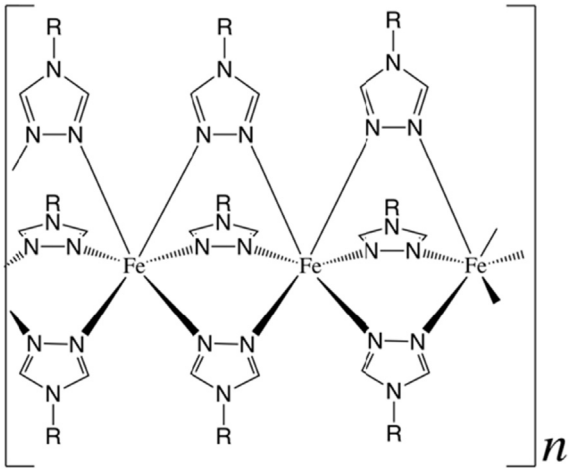

Fig. 6. Scheme of the triazole-bridged Fe^{II} 1D chains. Structural base for most triazole-based SCO coordination polymers.

Another interesting research line is the use of these robust materials as components for multifunctional composites in the search for synergy. The most relevant results were found in combination with organic conductors [93] and elastic polymers [94], where the spin transition triggers (and switches) the polymer properties. The latter case is particularly appealing since it opens a new field of application for SCO compounds as components for actuators [95].

Optical activity has also been introduced in this family, by using a chiral anion to neutralize the charge of the cationic chains [96]. Synergy between both properties generates switchable chiro-optical features. Additionally, this strategy also promotes molecular recognition. For instance, $[Fe(L37)_3](R\text{-}CSA)$ (**43**; L37 = 4-amino-1,2,4-triazole; R-CSA = R-camphorsulfonate) is sensitive to the inclusion of chiral guests [97]. Although changes in transition temperatures are small (<2 K), it was concluded that this material can distinguish between R- or S-2-butanol, as detected by magnetic or spectroscopic techniques.

Some interesting attempts to improve the processability of these materials have been reported recently. For example, films of $[Fe(L38)_3](DBS)_2$ (**44**; DBS = 4-dodecylbenzenesulfonate; L38 = 4-dodecaoctyl-1,2,4-triazole), possessing triazole ligands substituted with long alkyl chains, can be spin-coated from a homogeneous suspension in common solvents. The presence of long alkyl chains decreases cooperativity, but room temperature bistability is maintained [7]. This technique also allowed for the processing of thermochromic fibers [98].

Substitution at the N4 position with other groups, such as alkylcarboxylates, was also of interest. The use of ethyl-1,2,4-triazol-4-yl-propionate (L39) yielded the first case of a two-step spin transition in these compounds in the corresponding salt $[Fe(L39)_3](BF_4)_2$ (**45**) [99]. With the related ligand ethyl-*4H*-1,2,4-triazol-4-yl-acetate (L40), a complete $[Fe(L40)_3]X_2 \cdot xS$ (**46**; X = various anions; S = solvent) series was obtained, by tuning the memory effect at, below and above room temperature with different anions and solvent contents. The widest thermal hysteresis of 60 K was found for NO_3^-, on a solvent free derivative [100].

The robust and reliable spin transition of these 1D derivatives has also been exploited for the preparation of a variety of sensors. For example, a pressure sensor was developed with $[Fe(L41)_3]I_2 \cdot H_2O$ (**47**; L41 = 4-(2′-hydroxyethyl)-1,2,4-triazole) [101].

2.3.2. Polymers with cyanide ligands

Cyanometallates (Fig. 7) have been very useful building blocks for the development of molecule-based materials due to their double function. On the one hand, they act as multidentate ligands of transition metal cations via the N-end of the cyanide moieties; at the same time, they act as functional units, due to their electro-active metal-cores. The combination of cyanometallates with a second metal cation yields the large family of Prussian blue (PB) derivatives [102]: an extended family of three-dimensional coordination polymers. The extreme ligand field

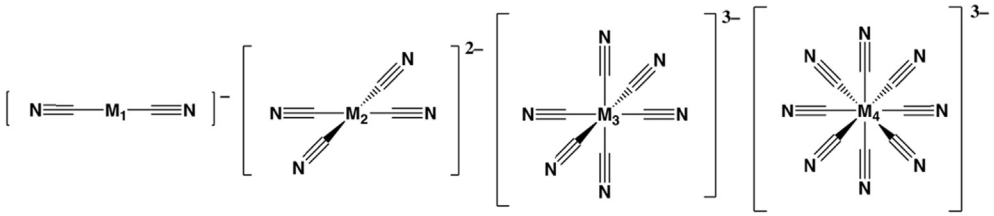

Fig. 7. Cyanometallate bridging ligands for the construction of spin crossover polymers. M1 = Ag, Au; M2 = Ni, Pd, Pt; M3 = Fe, Co; M4 = Nb.

difference between both ends of the cyanide ligand, i.e. a very strong field at the C-end and a weak one at the N-end, has not promoted the appearance of SCO in pure PB analogs, although some of them show SCO-related phenomena involving charge transfer processes [103].

The structure of these materials can be tuned by incorporation of additional ligands, which break the 3D network and, more importantly, modify the crystal field around the second metal cation. This strategy was very successful for the development of spin crossover materials. The first examples appeared by combining square planar tetracyanometallates, $[M(CN)_4]^{n-}$ and Fe(II) salts, with bridging N-heterocycles, such as pyrazine (L42). In these clathrates, Fe^{II} octahedral centers are coordinated by four weak ligands (cyanometallates) on the equatorial positions and by two relatively strong field ligands (e.g., pyrazine) at the axial positions, connecting two adjacent layers. This combination forms a 3D network (Fig. 8) exhibiting a cooperative spin transition [104–106], even as nanoparticles (<2 nm) [107,108]. Very fast spin transitions (≈20 ps) have been found in nanocrystals of the classical compound [Fe(L42)$Pt(CN)_4$] (**48**), with dimensions below 25 nm [109]. This confirms that SCO transitions may be fast enough for applications in information storage.

One of the most interesting prospects for these materials is the possibility to switch between spin states at high temperatures through electromagnetic irradiation. Through a mechanism different to the LIESST phenomena, these materials have shown light-controlled bistability within the thermal hysteresis cycle [110–112].

One of the most recent developments was the observation of a four-step spin crossover in [Fe(L43)$(Au(CN)_2)_2$]·*x*EtOH (**49**; L43 = 3,6-bis(4-pyridyl)-1,2-diazine) [113]. Remarkably, this compound can be obtained from its components, but also from post-functionalization of a preformed derivative, by a solid state reaction [114]. It is also worthy to mention that all Fe ions are crystallographically equivalent in the full HS or LS states, but the compound changes the lattice and periodicity to stabilize multiple phases with nonequivalent Fe(II) sites of variable LS/HS ratios. Theoretically, multistep switchable cooperative solids could open the way for three- or multi-bit electronics [115], and this family of materials is particularly prone to this phenomenon. A three-step transition was also found in the related clathrate [Fe(L44)$Pt(CN)_4$] (**50**; L44 = S,S′-bis-(4-pyridyl)methylenedithiolate) [116].

The record spin transition temperature for these materials was obtained for [Fe(L42)$(Au(CN)_2)_2$] (**51**), an interpenetrated solvent free 3D network [117]. This dense structure exhibits an 18 K wide hysteresis loop above 340 K. The isostructural silver analog [Fe(L42)$(Ag(CN)_2)_2$] (**52**) was reported as diamagnetic at room temperature [118]. Very recently, desolvation was shown to be crucial for **52** to exhibit a magnetic bistability very similar to that of the Au compound [119].

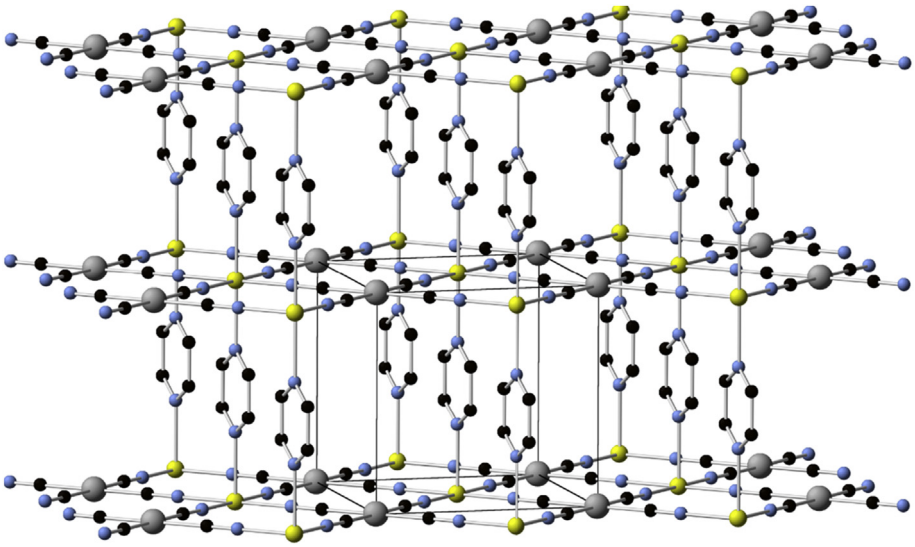

Fig. 8. 3D network in the [Fe(L42)$Pt(CN)_4$] (**48**) crystal structure (Fe, yellow; Pt, grey; C, black; N, light blue. H-atoms are omitted for clarity) [109].

When the bridging bis-monodentate ligand is long enough, interpenetrated 3D structures are typically obtained. An interpenetrated 3D network was found for the series $[Fe(L45)_2(Au(CN)_2)_2]\cdot(GM)$ (**53**; L45 = 2,5-bis(pyrid-4-yl)pyridine; GM = guest molecule). Ligand L45 has an uncoordinated nitrogen atom that acts as an H acceptor. The hysteretic transition of this material is extremely sensitive to the guest molecules, with tunable transition temperatures over a 130 K wide range, being lower for non-polar guests ($T_{1/2}$ > 120 K for *GM* = cyclohexane) and higher for polar guests ($T_{1/2}$ > 250 K for *GM* = isopropanol) [120].

Flexible ligands, such as *N*,*N*′-bis(4-pyridylmethyl) piperazine (L46), yield interpenetrated 3D polymers with linear $[M(CN)_2]^-$ dicyanometallates, $[Fe(L46)(M(CN)_2)_2]$ (M = Au, **54**; Ag, **55**), but not with the square planar $[Ni(CN)_4]^{2-}$. The interpenetrated networks show SCO behavior, while the Ni analog is an HS compound [121].

As mentioned above, the robust 3D structure of these clathrates, allows for reversible incorporation of guest molecules into their porous structure. Guest effects have also been recently reviewed [122]. An interesting approach, regarding the effect of guest molecules on the magnetic features, is the use of functional molecules, which can be further modified *in situ* to tune the transition. This was achieved by incorporation of maleic anhydride into the classic $[Fe(L42)Pt(CN)_4]$ (**48**) clathrates. A humid atmosphere easily hydrolyzes the anhydride yielding maleic acid, while the reverse transformation can be induced by heating. This allows controlling the spin transition from 275 K for the empty material, down to 200/170 K (2-step) for the anhydride guest, and to 150 K (incomplete) for the acid guest [123].

Guest effects were also studied for the expanded framework $[Fe(L23)Pt(CN)_4]$ (**56**). This material can host relatively large molecules, such as stilbene. The guest molecule also affects the magnetic properties, which has been ascribed to the flexibility of the bridging ligand [124]. The expanded 3D network $[Fe(L47)(Au(CN)_2)_2]$ (**57**; L47 = 1,4-bis(4-pyridyl)benzene) is especially sensitive to aromatic guests, with a record 73 K wide thermal hysteresis when naphthalene is incorporated into this porous structure. Comparatively, no hysteresis is observed when hosting simple benzene molecules instead [125].

Another guest-sensitive 3D polymer is $[Fe(L20)(Au(CN)_2)_2]$ (**58**). The cubic holes in this structure can be occupied by a variety of organic molecules, from benzene to *p*-xylene. This small modification in the size of the guest promotes a change in the spin transition of over 30 K. The transition temperature decreases by 50 K when the aromatic guest is substituted by chloroform, another fine example of the subtlety of spin transition phenomena [126]. The related compound $[Fe(L20)Ni(CN)_4]$ (**59**) is also sensitive to ethanol or acetone vapors, changing from two-step to one-step spin transitions upon absorption of these molecules [127].

Tris-monodentate ligands have also yielded 3D polymers with dicyanometallates. In this case, pillared structures are formed with hexagonal planes linked by the dicyanometallates, yielding porous structures [128]. $[Fe(L48)_{2/3}(M^I(CN)_2)_2]$ (**60**; L48 = 2,4,6-tris(4-pyridyl)-1,3,5-triazine; M^I = Ag, Au) for instance, can reversibly incorporate aromatic rings. It is remarkable that five membered rings of almost identical sizes (furan, pyrrole and thiophene) can be distinguished by these clathrates, resulting in modifications of up to 60 K in $T_{1/2}$ [129].

Enhanced porosity has been achieved with extremely long bis-monodentate ligands, such as 1,4-bis(4-pyridylethynyl)benzene (L49), as in the frameworks $[Fe(L49)M(CN)_4]$ (M = Pt, **61**; Pd, **62**; Ni, **63**). The host–guest chemistry of these materials has not been exploited yet, but promising results are envisioned in light of the effect observed preliminary on SCO features upon solvation/desolvation of solvents [130].

Analogous clathrates were also obtained with the planar $[Pd^{II}(SCN)_4]^{2-}$ anions. For example, $[Fe(L42)Pd(SCN)_4]$ (**64**) is HS at all temperatures at ambient pressure, due to a weaker ligand field with respect to $[Pd^{II}(CN)_4]^{2-}$. Under pressure, the spin transition behavior appears, resulting in an almost complete transition above 0.9 GPa [131].

The use of substituted pyrazines, such as 2-fluoropyrazine (L50), also yields the classic pillared 3D structure [132]. An interpenetrated 3D network was obtained as $[Fe(L50)(Au(CN)_2)_2]$ (**65**), showing a robust 40 K wide hysteresis cycle, in the 220–270 K range. However, depending on preparation conditions, L50 may also act as a terminal ligand. Terminal ligands (Fig. 4), such as pyridine (CL6) [133,134], occupy the axial positions, isolating the cyanide-bridged tetragonal 2D network. These layered structures have also shown interesting spin crossover phenomena.

The L50 analogs, chloro- and 2-methyl-pyrazine (CL7, CL8), only yield 2D networks, acting as pyridine-like terminal ligands, as in $[Fe(CL7)_2M(CN)_4]$ (**66**, M = Ni, Pd, Pt; Fig. 9) [135]. All these materials show spin transition with significant thermal hysteresis cycles, up to 30 K wide. The 3-aminopyridine (CL9) case is interesting because it is

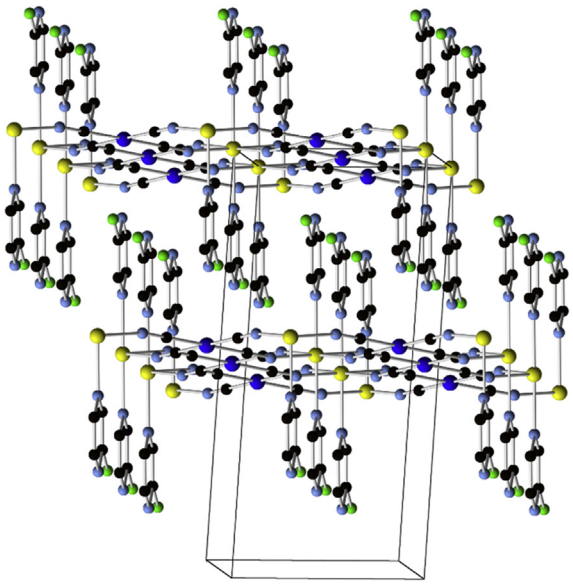

Fig. 9. 2D network in the $[Fe(CL7)_2Ni(CN)_4]$ (**66**) crystal structure. (Fe, yellow; Ni, deep blue; C, black; N, light blue; Cl, green. H-atoms are omitted for clarity) [135].

particularly sensitive to the Ni, Pd or Pt component, modifying the hysteresis in width (from 27 to 37 K) and position (from 150 up to 190 K) [136]. Hydrogen bonding promoted by the amine group was identified to be responsible for the enhanced cooperativity in these compounds. 4-X-Pyridine (CL10), where X is Cl, Br or I, yields 2D isostructural coordination polymers with $[Au(CN)_2]$, e.g., $[Fe(CL10)_2((Au(CN)_2)_2]$ (**67**; X = Cl), exhibiting a significant effect of the halide on the spin transition cooperativity, from abrupt to gradual [137]. A lower transition temperature and no hysteresis were found, for example, on the compound $[Fe(CL11)_2(Au(CN)_2)_2]$ (**68**; CL11 = 4-(3-pentyl) pyridine), with a large aliphatic substituent on the pyridine-like ligand [138].

Some 1,2,4-triazole ligands may also act as terminal ligands in combination with cyanometallates to yield 2D networks. This is the case of L3 in the 2D material $[Fe(L3)_2Pt(CN)_4]$ (**69**). The L3 ligands are interdigitated between layers, creating two nonequivalent Fe(II) sites. There is a first order spin transition from a fully HS state to an intermediate LS–HS state, while the ground LS–LS state can only be accessed via the reverse-LIESST effect. The strong metastability of the intermediate state was correlated to the antiferroelastic interactions between layers [139].

A two dimensional network was also obtained with 5-methyl-2-(thienyl)vinyl-1,2,4-triazole (CL12) [140]. This ligand occupies the axial positions of the Fe(II) centers in $[Fe(CL12)_2Pd(CN)_4]\cdot nH_2O$ (**70**). This material is an HS compound in the hydrated form, but an abrupt transition with an $\approx$20 K wide hysteresis appears upon dehydration. A spin transition can also be induced under pressure, but in this case, a two-step transition is induced. This illustrates the importance of the crystallographic transitions associated with SCO phenomena when it comes to promoting cooperativity.

If bis-dentate chelating ligands (instead of bismonodentate bridging ligands) are combined with $[M(CN)_4]^{2-}$ moieties, the formation of a 3D or 2D structure is precluded, and 1D polymers are obtained. This is the case, for example, with 2-picolylamine (CL13) or 2-(1*H*-pyrazol-3-yl)-pyridine (CL14). The corresponding zig zag chains $[Fe(CL13)_2M(CN)_4]$ (**71**, Fig. 10) and $[Fe(CL14)_2M(CN)_4]$ (**72**; M = Pd, Pt) exhibit abrupt spin transitions between 100 K and 300 K depending on the solvent and counter anions [141]. Only very narrow hysteresis was found in all these materials.

1D polymers are obtained with 4-amino-3,5-bis(pyridine-2-yl)-1,2,4-triazole (CL15) with formula $[Fe(CL15)_2M(CN)_4]$ (**73**; M = Pt, Ni). In this structure, the two CL15 ligands occupy the equatorial positions, and the chain grows through the $M(CN)_4$ bridging axial positions in *trans*. These chains are LS at room temperature while the HS is populated above 300 K. Decomposition occurs before the transition is complete [142,143].

Most examples described so far were obtained with linear dicyanometallates or square planar tetracyanometalates. Fewer examples of cyanometallates with higher coordination numbers have been reported. However, a remarkable example has been unveiled with an octacyanometallate and the ancillary ligand 4-pyridinealdoxime (CL16); $[Fe_2(CL16)_8Nb(CN)_8]$ (**74**) [144]. The spin transition here is gradual, between 100 and 200 K. An unprecedented phenomenon occurs at low *T*, where the compound shows the LIESST effect. Population of the HS state via irradiation triggers ferromagnetic exchange between both types of metals. As a result of this, the material becomes a molecular base magnet exhibiting magnetic hysteresis. This represented the first reported LIESST-promoted magnetic ordering. Following this work, analogous phenomena were also observed using the simple pyrazole ligand (CL17), in $[Fe_2(CL17)_8Nb(CN)_8]\cdot 4H_2O$ (**75**) [145], although in this case the spin-crossover is pressure-induced. Another ligand that promotes SCO phenomena in octacyanide-based coordination polymers is (2-pyridyl)methanol (CL18), which leads to $[Fe_2(CL18)_8W(CN)_8]\cdot nH_2O$ (**76**). In this case, only two positions on the Fe centers are occupied by CN ligands [146].

2.3.3. Other ligands

There are few bridging ligands that are able to form binary (ML_n) coordination networks when combined with metal centers, providing ligand fields of the appropriate strength to bring bistability with a simple ML_6 coordination mode. The 1,2,4-triazole ligand is a major example, as described in Section 2.3.1.

One interesting 1D chain is obtained with the rigid ligand 1,4-bis(tetrazol-1-ylmethyl)benzene (L51), which forms triple bridges between octahedral Fe(II) centers. The shape of this ligand creates a porous structure, $[Fe(L51)_3](ClO_4)_2$ (**77**), that recognizes CO_2 molecules [147]. The inclusion of these molecules from the gas phase induces a minor change (but measurable) in $T_{1/2}$. When this polymer is diluted in the solid state with the structurally analogous bis-triazole (L52), the different ligand field brings $T_{1/2}$ from 200 K for the pure tetrazole compound

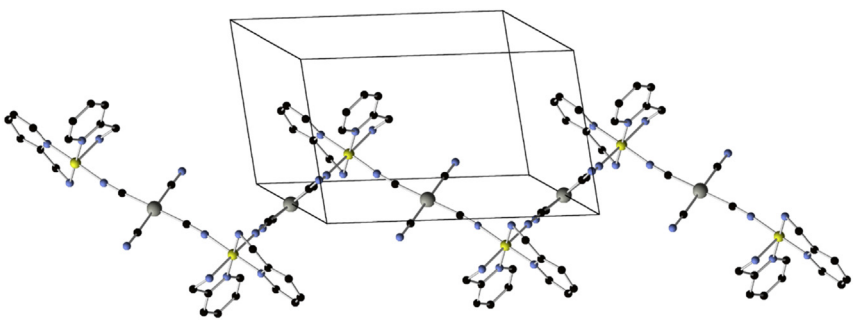

Fig. 10. 1D network in the $[Fe(CL13)_2Pd(CN)_4]$ (**71**) crystal structure. (Fe, yellow; Pd, grey; C, black; N, light blue; Cl, green. H-atoms are omitted for clarity) [141].

down to 60 K for the solid solution (ratio 2/1). The all triazole compound $[Fe(L52)_3](ClO_4)_2$ (**78**) is HS [148].

Ligand 1,3-di(tetrazol-1-yl)propane (L53), analogous to L51 with substitution of the benzene ring by a flexible alkyl chain, also forms 1D chains with the formula $[Fe(L53)_3]X_2$ (**79**; X = ClO_4^- or BF_4^-), which show abrupt spin transitions but no hysteresis. An efficient LIESST effect was observed [149]. Several analogous 1,ω-di(azolyl)alkane-type ligands (L54) yield cationic 2D networks $[Fe(L54)_3]^{2+}$ (**80**), typically with incomplete or gradual spin transitions, due to the flexibility/elasticity of the alkane chain [150]. The latter remains crystallographically disordered in the HS or the LS state, even under pressure or after light-induced transitions at very low temperature.

6,6′-Bis(1*H*-tetrazol-5-yl)-2-2′-bipyridine (L55) is a multidentate ligand that yields a 2D neutral network [Fe(L55)] (**81**) upon complete deprotonation [151], with the axial positions occupied by tetrazole units from adjacent complexes. This tetragonal network shows an abrupt spin transition and complete LIESST effect at 10 K, revealing antiferromagnetic interactions between Fe(II) centers. Tetrazole-2-yl rings have also been combined with axially coordinated nitriles yielding 2D networks, with gradual SCO and an effective LIESST effect [152].

A two-dimensional tetragonal grid was obtained with 3-(5-bromo-2-pyridyl)-5-(4-pyridil)-1,2,4-triazole (L56), of the composition $[Fe(L56)_2]$ (**82**), showing a 2-step spin transition. The flexibility of this network makes it sensitive to guest molecules and pressure, showing easy tuning of the SCO features [153].

Another type of coordination polymer is obtained with *trans*-4,4′-azo-1,2,4-triazole (L57), $[Fe(L57)_3]X_2$ (**83**, X = ClO_4^- or BF_4^-), with a spin transition close to room temperature [154]. These interpenetrated 3D networks are sensitive to humidity, which makes this transition more gradual and lowers the $T_{1/2}$ values.

3,5-Substituted triazole ligands functionalized with pyridine groups, such as 3-(2-pyridyl)-5-(3-pyridyl)-1,2,4-triazole (L58), 2-(5-(4-(1*H*-imidazole-1yl)phenyl)-4*H*-1,2,4-triazol-3-yl)pyridine (L59), or 2-(5-(4-(pyridine-3-yl) phenyl)-4*H*-1,2,4-triazol-3-yl)-pyridine (L60), yield a series of solvent-free robust 2D Fe networks upon ligand deprotonation: $[Fe(L58)_2]$ (**84**), $[Fe(L59)_2]$ (**85**) and $[Fe(L60)_2]$ (**86**). These ligands possess a monodentate pyridyl or imidazolyl site in addition to the triazol-pyridyl chelating site, while their anionic nature avoids the need for counter anions. These coordination networks exhibit very high (gradual and incomplete) spin transition temperatures. Compound **83** features the highest $T_{1/2}$ spin transition ever reported (≥500 K) [155,156], thanks to their extremely high thermal stability.

Many other examples of SCO coordination networks are based on the combination of two different ligand types, one bridging and one capping. This reduces dimensionality, but increases the structural and chemical versatility. One of the most successful strategies is based on the combination of bispyridine-like ligands with NCS^- (or $NCSe^-$) anions, as capping ligands. For example, 1,2-bis(pyridine-4-ylmethylene)hydrazine (L61) creates porous materials of the formula $[Fe(L61)_2(NCX)_2]$ (**87**), where the spin transition is highly dependent on guest molecules [157]. These materials tend to exhibit interpenetration, with the grid-like planes in two orthogonal directions. The same is observed for 1,4-bis(pyridin-4-yl) benzene (L47) in $[Fe(L47)_2(NCX)_2]$ (**88**) compounds. Substitution with the isoelectronic $NCBH_3^-$ anion slightly modifies the packing of the 2D layers and increases the spin transition temperatures of the corresponding $[Fe(L47)_2(NCBH_3)_2]$ (**89**) polymers by 100 K [158]. Surprisingly, the analogous structure with L20, obtained with water groups substituting the NCX^- anions, $[Fe(L20)_2(H_2O)_2](ClO_4)_2$ (**90**), has been reported to exhibit a spin transition, being one of the few examples where an Fe^{II} coordination material with weak ligand field water molecules shows SCO phenomena [159].

Particularly interesting is the series of 2D interpenetrating networks obtained from *trans*-(4,4′-vinylenedipyridine (L22) [160] with formula $[Fe(L22)_2(SCN)_2]\cdot GM$ (**91**), where GM may be a variety of guest molecules. A detailed study on the effect of GM on the SCO properties indicates that the transition temperature is almost invariable, but the different sizes and nature of the ligands have strong influence on the cooperativity, promoting the appearance of small hysteresis [161]. In related work, poly-4-vinylpyridine and its block copolymers have been used as a nucleation matrix to template nanoparticle synthesis of coordination polymers, resulting in increased stability against degradation and excellent size control [162,163].

Tris-monodentate ligands, such as 1,3,5-tris(4-pyridyl) benzene (L62), create a 3D structure (boracite-like) of formula $[(Fe(NCS)_2)_3(L62)_4]$ (**92**), with octahedral $Fe(N_4)(SCN)_2$ building blocks. This porous network shows an incomplete transition around 150 K, with little dependence on the nature of the guest molecules [164]. The tris-chelating ligand 1,4,5,8,9,19-hexazatriphenylene (L63) forms a 1D coordination polymer. Only two of the three chelating positions are binding to Fe(II) centers, creating a homochiral structure with formula $[Fe(L63)(NCS)_2]$ (**93**) that exhibits a two-step spin transition [165].

The zigzag chain, $[Fe(CL19)(L64)](BPh_4)_2$ (**94**), is obtained with 1,2-bis(pyridine-2-yl-methyl)thio]ethane (CL19) and the linker adiponitrile (L64) [166]. Again, a solvent dependent behavior was observed, as is often seen in 1D systems. The counter anion is also important to favor the polymeric structure, since bulky inorganic anions such as SbF_6^- induce crystallization of an LS discrete dimer.

The combination of a salen-type (CL3) Fe^{II} complex and the bridging ligand 4,4′-dipyridylethyne (L21) gives 1D polymers, [Fe(CL3)(L21)] (**95**), with solvent-dependent SCO behavior. When desolvated, these materials exhibit a three-step spin transition [62]. Analogous 1D polymers have been reported for 3,3′-azopyridine (L65) as [Fe(CL3)(L65)] (**96**), which shows a very slow transition, favoring trapping of the HS state via fast cooling [167].

The ligand tetra(4-pyridyl)tetrathiafulvalene (L66) was especially designed to incorporate multiple properties into an Fe^{II} coordination network, including spin transition. With additional dicyanamide (L67) bridging ligands, a 3D coordination network was obtained, $[Fe(L66)(L67)](ClO_4)$ (**97**), exhibiting spin transition ($T_{1/2}$ = 146 K), the LIESST effect, redox activity and enhanced conductivity upon oxidative doping [168].

There are few exceptions to the Fe^{II} paradigm in SCO coordination polymers. Only a small number of Co^{II} coordination networks belong to this family. The compound $[CoX_2(L68)]$ (**98**; X = Cl, Br) is one of the few non-iron SCO examples. Ligand L68 was particularly designed for the formation of 1D linear chains, with two opposite and different coordination sites. The SCO is solvent dependent, and shows no thermal memory effect [169].

Another SCO 1D chain was obtained with the equatorial (N_4) ligand N–N′-(bis(pyridine-2-yl)benzylidine)ethane-1,2-diamine (CL20) with bridging L67. These chains are very sensitive to the nature of the counterions: abrupt with hysteresis in the case of ClO_4^- [170] and gradual in the case of PF_6^- [171].

3. Conclusions

This revision shows that SCO research continues to attract great interest. One of the pillars of progress in this field is synthetic chemistry, which is the source of its objects of study. The library of SCO compounds have enabled us to gather fundamental knowledge about this property and will be paramount to implement potential applications. It becomes very clear in this manuscript that the production of novel SCO polynuclear complexes has remained a very prolific activity during the last few years.

The use of new ligands and a combination of new and old organic linkers is paramount in order to unveil new aspects of the SCO phenomenon as well as for the ambitious goal of combining the spin switching property with other molecular functions. As described in this paper, we have found that the major research lines in multinuclear SCO materials are built towards several major objectives. As expected and predicted in our introduction, multi-step transitions and high temperature bistability keep moving the field further. In addition, recent literature has brought some additional and unique opportunities for these compounds. On the one hand, the promising appearance of dynamic effects (slow relaxation from the HS excited state) in these systems opens the possible development of SCO-based single-molecule memories while, in the past, the memory effect was exclusively associated with bulk materials. Another fascinating possibility is the processing of these polynuclear molecules or coordination networks as nanostructures (monolayers or thin films). The combination of these two recent developments is one of the challenges for molecular magnetism and coordination chemistry. Polynuclear entities with the memory effect at the nano-scale, at technologically relevant temperatures, remain one of the holy grails in molecular magnetism. In our opinion, polynuclear SCO is the most promising system to achieve such a target in the near future.

References

[1] P. Gütlich, A.B. Gaspar, Y. Garcia, Beilstein J. Org. Chem. 9 (2013) 342–391.
[2] A. Urtizberea, O. Roubeau, Chem. Sci. 8 (2017) 2290–2295.
[3] Y. Jiao, J.P. Zhu, Y. Guo, W.J. He, Z.J. Guo, J. Mater. Chem. C 5 (2017) 5214–5222.
[4] G.A. Craig, J.S. Costa, O. Roubeau, S.J. Teat, H.J. Shepherd, M. Lopes, G. Molnár, A. Bousseksou, G. Aromí, Dalton Trans. 43 (2014) 729–737.
[5] F. Guillaume, Y.A. Tobon, S. Bonhommeau, J.F. Letard, L. Moulet, E. Freysz, Chem. Phys. Lett. 604 (2014) 105–109.
[6] C. Faulmann, K. Jacob, S. Dorbes, S. Lampert, I. Malfant, M.L. Doublet, L. Valade, J.A. Real, Inorg. Chem. 46 (2007) 8548–8559.
[7] G. Bovo, I. Braunlich, W.R. Caseri, N. Stingelin, T.D. Anthopoulos, K.G. Sandeman, D.D.C. Bradley, P.N. Stavrinou, J. Mater. Chem. C 4 (2016) 6240–6248.
[8] A. Diaconu, S.L. Lupu, I. Rusu, I.M. Risca, L. Salmon, G. Molnár, A. Bousseksou, P. Demont, A. Rotaru, J. Phys. Chem. Lett. 8 (2017) 3147–3151.
[9] A. Iazzolino, G. Galle, J. Degert, J.F. Létard, E. Freysz, Chem. Phys. Lett. 641 (2015) 14–19.
[10] P.L. Holland, Acc. Chem. Res. 48 (2015) 1696–1702.
[11] S. Samanta, S. Demesko, S. Dechert, F. Meyer, Angew. Chem. Int. Ed. 54 (2015) 583–587.
[12] M.A. Halcrow, Chem. Soc. Rev. 40 (2011) 4119–4142.
[13] M.A. Halcrow, Chem. Lett. 43 (2014) 1178–1188.
[14] J. Olguín, S. Brooker, in: Spin-crossover Materials, John Wiley & Sons Ltd, 2013, pp. 77–120.
[15] M. Carmen Muñoz, J. Antonio Real, in: Spin-crossover Materials, John Wiley & Sons Ltd, 2013, pp. 121–146.
[16] G. Aromí, L.A. Barrios, O. Roubeau, P. Gamez, Coord. Chem. Rev. 255 (2011) 485–546.
[17] J. Olguín, S. Brooker, Coord. Chem. Rev. 255 (2011) 203–240.
[18] O. Roubeau, Chem. Eur J. 18 (2012) 15230–15244.
[19] M.A. Halcrow, Coord. Chem. Rev. 253 (2009) 2493–2514.
[20] G.A. Craig, O. Roubeau, G. Aromí, Coord. Chem. Rev. 269 (2014) 13–31.
[21] B. Weber, in: Spin-crossover Materials, John Wiley & Sons Ltd, 2013, pp. 55–76.
[22] A. Real, J. Zarembowitch, O. Kahn, X. Solans, Inorg. Chem. 26 (1987) 2939–2943.
[23] S. Zein, S.A. Borshch, J. Am. Chem. Soc. 127 (2005) 16197–16201.
[24] R. Kulmaczewski, J. Olguín, J.A. Kitchen, H.L.C. Feltham, G.N.L. Jameson, J.L. Tallon, S. Brooker, J. Am. Chem. Soc. 136 (2014) 878–881.
[25] E.D. Doidge, J.W. Roebuck, M.R. Healy, P.A. Tasker, Coord. Chem. Rev. 288 (2015) 98–117.
[26] J.J.A. Kolnaar, M. I. d. Heer, H. Kooijman, A.L. Spek, G. Schmitt, V. Ksenofontov, P. Gütlich, J.G. Haasnoot, J. Reedijk, Eur. J. Inorg. Chem. 1999 (1999) 881–886.
[27] Y. Garcia, F. Robert, A.D. Naik, G. Zhou, B. Tinant, K. Robeyns, S. Michotte, L. Piraux, J. Am. Chem. Soc. 133 (2011) 15850–15853.
[28] O. Roubeau, P. Gamez, S.J. Teat, Eur. J. Inorg. Chem. 2013 (2013) 934–942.
[29] B. Ding, Y.Y. Liu, Y. Wang, J.-G. Ma, Z. Niu, W. Shi, P. Cheng, Inorg. Chem. Commun. 31 (2013) 44–48.
[30] X.X. Wu, Y.Y. Wang, P. Yang, Y.Y. Xu, J.Z. Huo, B. Ding, Y. Wang, X. Wang, Cryst. Growth Des. 14 (2014) 477–490.
[31] X. Cheng, Q. Yang, C. Gao, B.-W. Wang, T. Shiga, H. Oshio, Z.-M. Wang, S. Gao, Dalton Trans. 44 (2015) 11282–11285.
[32] B.A. Leita, B. Moubaraki, K.S. Murray, J.P. Smith, J.D. Cashion, Chem. Commun. (2004) 156–157.
[33] K. Nakano, N. Suemura, S. Kawata, A. Fuyuhiro, T. Yagi, S. Nasu, S. Morimoto, S. Kaizaki, Dalton Trans. (2004) 982–988.
[34] K. Nakano, S. Kawata, K. Yoneda, A. Fuyuhiro, T. Yagi, S. Nasu, S. Morimoto, S. Kaizaki, Chem. Commun. (2004) 2892–2893.
[35] K. Nakano, N. Suemura, K. Yoneda, S. Kawata, S. Kaizaki, Dalton Trans. (2005) 740–743.
[36] C.J. Schneider, J.D. Cashion, B. Moubaraki, S.M. Neville, S.R. Batten, D.R. Turner, K.S. Murray, Polyhedron 26 (2007) 1764–1772.
[37] M. Sy, F. Varret, K. Boukheddaden, G. Bouchez, J. Marrot, S. Kawata, S. Kaizaki, Angew. Chem. Int. Ed. 53 (2014) 7539–7542.
[38] C.J. Schneider, J.D. Cashion, N.F. Chilton, C. Etrillard, M. Fuentealba, J.A.K. Howard, J.-F. Létard, C. Milsmann, B. Moubaraki, H.A. Sparkes, S.R. Batten, K.S. Murray, Eur. J. Inorg. Chem. 2013 (2013) 850–864.
[39] S. Rodríguez-Jiménez, H.L.C. Feltham, S. Brooker, Angew. Chem. Int. Ed. 55 (2016) 15067–15071.
[40] J.S. Costa, S. Rodriguez-Jimenez, G.A. Craig, B. Barth, C.M. Beavers, S.J. Teat, G. Aromi, J. Am. Chem. Soc. 136 (2014) 3869–3874.
[41] J.A. Kitchen, N.G. White, G.N.L. Jameson, J.L. Tallon, S. Brooker, Inorg. Chem. 50 (2011) 4586–4597.
[42] J.A. Kitchen, J. Olguín, R. Kulmaczewski, N.G. White, V.A. Milway, G.N.L. Jameson, J.L. Tallon, S. Brooker, Inorg. Chem. 52 (2013) 11185–11199.
[43] R.W. Hogue, H.L.C. Feltham, R.G. Miller, S. Brooker, Inorg. Chem. 55 (2016) 4152–4165.
[44] C.F. Herold, S.I. Shylin, E. Rentschler, Inorg. Chem. 55 (2016) 6414–6419.
[45] C. Köhler, E. Rentschler, Eur. J. Inorg. Chem. 2016 (2016) 1955–1960.

[46] R.W. Saalfrank, H. Maid, A. Scheurer, Angew. Chem. Int. Ed. 47 (2008) 8794–8824.
[47] C. Piguet, G. Bernardinelli, G. Hopfgartner, Chem. Rev. 97 (1997) 2005–2062.
[48] F. Tuna, M.R. Lees, G.J. Clarkson, M.J. Hannon, Chem. Eur J. 10 (2004) 5737–5750.
[49] D. Pelleteret, R. Clérac, C. Mathonière, E. Harte, W. Schmitt, P.E. Kruger, Chem. Commun. (2009) 221–223.
[50] N. Struch, J.G. Brandenburg, G. Schnakenburg, N. Wagner, J. Beck, S. Grimme, A. Lützen, Eur. J. Inorg. Chem. 2015 (2015) 5503–5510.
[51] C.S. Hawes, C.M. Fitchett, P.E. Kruger, Supramol. Chem. 24 (2012) 553–562.
[52] H. Hagiwara, T. Tanaka, S. Hora, Dalton Trans. 45 (2016) 17132–17140.
[53] H. Phan, J.J. Hrudka, D. Igimbayeva, L.M. Lawson Daku, M. Shatruk, J. Am. Chem. Soc. 139 (2017) 6437–6447.
[54] M. Darawsheh, L.A. Barrios, O. Roubeau, S.J. Teat, G. Aromí, Chem. Eur J. 22 (2016) 8635–8645.
[55] M.D. Darawsheh, L.A. Barrios, O. Roubeau, S.J. Teat, G. Aromí, Chem. Commun. 53 (2017) 569–572.
[56] H. Takezawa, T. Murase, G. Resnati, P. Metrangolo, M. Fujita, Angew. Chem. Int. Ed. 54 (2015) 8411–8414.
[57] B. Icli, E. Solari, B. Kilbas, R. Scopelliti, K. Severin, Chem. Eur J. 18 (2012) 14867–14874.
[58] B.K. Roland, H.D. Selby, M.D. Carducci, Z. Zheng, J. Am. Chem. Soc. 124 (2002) 3222–3223.
[59] D. Aguila, L.A. Barrios, O. Roubeau, S.J. Teat, G. Aromi, Chem. Commun. 47 (2011) 707–709.
[60] D. Fedaoui, Y. Bouhadja, A. Kaiba, P. Guionneau, J.-F. Létard, P. Rosa, Eur. J. Inorg. Chem. 2008 (2008) 1022–1026.
[61] A.Y. Verat, N. Ould-Moussa, E. Jeanneau, B. Le Guennic, A. Bousseksou, S.A. Borshch, G.S. Matouzenko, Chem. Eur J. 15 (2009) 10070–10082.
[62] K. Dankhoff, C. Lochenie, F. Puchtler, B. Weber, Eur. J. Inorg. Chem. 2016 (2016) 2136–2143.
[63] G.S. Matouzenko, E. Jeanneau, A. Yu Verat, A. Bousseksou, Dalton Trans. 40 (2011) 9608–9618.
[64] G.S. Matouzenko, E. Jeanneau, A.Y. Verat, Y. de Gaetano, Eur. J. Inorg. Chem. 2012 (2012) 969–977.
[65] Y. de Gaetano, E. Jeanneau, A.Y. Verat, L. Rechignat, A. Bousseksou, G.S. Matouzenko, Eur. J. Inorg. Chem. 2013 (2013) 1015–1023.
[66] J.J.M. Amoore, C.J. Kepert, J.D. Cashion, B. Moubaraki, S.M. Neville, K.S. Murray, Chem. Eur J. 12 (2006) 8220–8227.
[67] J.J.M. Amoore, S.M. Neville, B. Moubaraki, S.S. Iremonger, K.S. Murray, J.-F. Létard, C.J. Kepert, Chem. Eur J. 16 (2010) 1973–1982.
[68] M. Quesada, P. de Hoog, P. Gamez, O. Roubeau, G. Aromi, B. Donnadieu, C. Massera, M. Lutz, A.L. Spek, J. Reedijk, Eur. J. Inorg. Chem. 2006 (2006) 1353–1361.
[69] S. Kanegawa, S. Kang, O. Sato, Eur. J. Inorg. Chem. 2013 (2013) 725–729.
[70] W.A. Gobeze, V.A. Milway, J. Olguín, G.N.L. Jameson, S. Brooker, Inorg. Chem. 51 (2012) 9056–9065.
[71] E. Milin, S. Belaïd, V. Patinec, S. Triki, G. Chastanet, M. Marchivie, Inorg. Chem. 55 (2016) 9038–9046.
[72] J.G. Park, I.-R. Jeon, T.D. Harris, Inorg. Chem. 54 (2015) 359–369.
[73] M. van der Meer, Y. Rechkemmer, F.D. Breitgoff, R. Marx, P. Neugebauer, U. Frank, J. van Slageren, B. Sarkar, Inorg. Chem. 55 (2016) 11944–11953.
[74] D. Savard, C. Cook, G.D. Enright, I. Korobkov, T.J. Burchell, M. Murugesu, CrystEngComm 13 (2011) 5190–5197.
[75] G. Vos, R.A.G. De Graaff, J.G. Haasnoot, A.M. Van der Kraan, P. De Vaal, J. Reedijk, Inorg. Chem. 23 (1984) 2905–2910.
[76] G. Vos, R.A. Le Febre, R.A.G. De Graaff, J.G. Haasnoot, J. Reedijk, J. Am. Chem. Soc. 105 (1983) 1682–1683.
[77] V. Gómez, J. Benet-Buchholz, E. Martin, J.R. Galán-Mascarós, Chem. Eur J. 20 (2014) 5369–5379.
[78] V. Gómez, C.S. de Pipaon, P. Maldonado-Illescas, J.C. Waerenborgh, E. Martin, J. Benet-Buchholz, J.R. Galán-Mascarós, J. Am. Chem. Soc. 137 (2015) 11924–11927.
[79] B. Schneider, S. Demeshko, S. Dechert, F. Meyer, Angew. Chem. Int. Ed. 49 (2010) 9274–9277.
[80] M. Steinert, B. Schneider, S. Dechert, S. Demeshko, F. Meyer, Angew. Chem. Int. Ed. 53 (2014) 6135–6139.
[81] J. Cirera, Rev. Inorg. Chem. 34 (2014) 199–216.
[82] A. Bousseksou, G. Molnár, L. Salmon, W. Nicolazzi, Chem. Soc. Rev. 40 (2011) 3313–3335.
[83] P. Gutlich, Eur. J. Inorg. Chem. 2013 (2013) 581–591.
[84] O. Kahn, C.J. Martinez, Science 279 (1998) 44–48.
[85] C. Bartual-Murgui, E. Natividad, O. Roubeau, J. Mater. Chem. C 3 (2015) 7916–7924.
[86] A. Grosjean, N. Daro, S. Pechev, L. Moulet, C. Etrillard, G. Chastanet, P. Guionneau, Eur. J. Inorg. Chem. 2016 (2016) 1961–1966.
[87] A. Urakawa, W. Van Beek, M. Monrabal-Capilla, J.R. Galán-Mascarós, L. Palin, M. Milanesio, J. Phys. Chem. C 115 (2011) 1323–1329.
[88] C.M. Quintero, G. Felix, I. Suleimanov, J.S. Costa, G. Molnár, L. Salmon, W. Nicolazzi, A. Bousseksou, Beilstein J. Nanotechnol. 5 (2014) 2230–2239.
[89] Y.X. Wang, D. Qiu, S.F. Xi, Z.D. Ding, Z.J. Li, Y.X. Li, X.H. Ren, Z.G. Gu, Chem. Commun. 52 (2016) 8034–8037.
[90] J. Dugay, M. Gimenez-Marques, T. Kozlova, H.W. Zandbergen, E. Coronado, H.S.J. van der Zant, Adv. Mater. 27 (2015) 1288–1293.
[91] J.R. Galán-Mascarós, E. Coronado, A. Forment-Aliaga, M. Monrabal-Capilla, E. Pinilla-Cienfuegos, M. Ceolin, Inorg. Chem. 49 (2010) 5706–5714.
[92] J.M. Herrera, S. Titos-Padilla, S.J.A. Pope, I. Berlanga, F. Zamora, J.J. Delgado, K.V. Kamenev, X. Wang, A. Prescimone, E.K. Brechin, E. Colacio, J. Mater. Chem. C 3 (2015) 7819–7829.
[93] Y.S. Koo, J.R. Galán-Mascarós, Adv. Mater. 26 (2014) 6785–6789.
[94] S. Rat, V. Nagy, I. Suleimanov, G. Molnar, L. Salmon, P. Demont, L. Csoka, A. Bousseksou, Chem. Commun. 52 (2016) 11267–11269.
[95] H.J. Shepherd, I.A. Gural'skiy, C.M. Quintero, S. Tricard, L. Salmon, G. Molnar, A. Bousseksou, Nature Commun. 4 (2013).
[96] I.A. Gural'skiy, V.A. Reshetnikov, A. Szebeszczyk, E. Gumienna-Kontecka, A.I. Marynin, S.I. Shylin, V. Ksenofontov, I.O. Fritsky, J. Mater. Chem. C 3 (2015) 4737–4741.
[97] I.A. Gural'skiy, O.I. Kucheriv, S.I. Shylin, V. Ksenofontov, R.A. Polunin, I.O. Fritsky, Chem. Eur J. 21 (2015) 18076–18079.
[98] I. Braunlich, S. Lienemann, C. Mair, P. Smith, W. Caseri, J. Mater. Sci. 50 (2015) 2355–2364.
[99] M.M. Dirtu, F. Schmit, A.D. Naik, I. Rusu, A. Rotaru, S. Rackwitz, J.A. Wolny, V. Schunemann, L. Spinu, Y. Garcia, Chem. Eur J. 21 (2015) 5843–5855.
[100] M.M. Dîrtu, A.D. Naik, A. Rotaru, L. Spinu, D. Poelman, Y. Garcia, Inorg. Chem. 55 (2016) 4278–4295.
[101] C.M. Jureschi, J. Linares, A. Rotaru, M.H. Ritti, M. Parlier, M.M. Dirtu, M. Wolff, Y. Garcia, Sensors 15 (2015) 2388–2398.
[102] N.R. de Tacconi, K. Rajeshwar, R.O. Lezna, Chem. Mater. 15 (2003) 3046–3062.
[103] D. Li, R. Clérac, O. Roubeau, E. Harté, C. Mathonière, R. Le Bris, S.M. Holmes, J. Am. Chem. Soc. 130 (2008) 252–258.
[104] V. Niel, J.M. Martínez-Agudo, M.C. Muñoz, A.B. Gaspar, J.A. Real, Inorg. Chem. 40 (2001) 3838–3839.
[105] M. Ohba, K. Yoneda, G. Agusti, M.C. Muñoz, A.B. Gaspar, J.A. Real, M. Yamasaki, H. Ando, Y. Nakao, S. Sakaki, S. Kitagawa, Angew. Chem. Int. Ed. 48 (2009) 4767–4771.
[106] C.H. Pham, J. Cirera, F. Paesani, J. Am. Chem. Soc. 138 (2016) 6123–6126.
[107] G. Félix, M. Mikolasek, H. Peng, W. Nicolazzi, G. Molnár, A.I. Chumakov, L. Salmon, A. Bousseksou, Phys. Rev. B 91 (2015), 024422.
[108] H.N. Peng, S. Tricard, G. Felix, G. Molnár, W. Nicolazzi, L. Salmon, A. Bousseksou, Angew. Chem. Int. Ed. 53 (2014) 10894–10898.
[109] D.M. Sagar, F.G. Baddour, P. Konold, J. Ullom, D.A. Ruddy, J.C. Johnson, R. Jimenez, J. Phys. Chem. Lett. 7 (2016) 148–153.
[110] S. Bonhommeau, G. Molnar, A. Galet, A. Zwick, J.A. Real, J.J. McGarvey, A. Bousseksou, Angew. Chem. Int. Ed. 44 (2005) 4069–4073.
[111] M. Castro, O. Roubeau, L. Piñeiro-López, J.A. Real, J.A. Rodríguez-Velamazán, J. Phys. Chem. C 119 (2015) 17334–17343.
[112] S. Cobo, D. Ostrovskii, S. Bonhommeau, L. Vendier, G. Molnár, L. Salmon, K. Tanaka, A. Bousseksou, J. Am. Chem. Soc. 130 (2008) 9019–9024.
[113] J.E. Clements, J.R. Price, S.M. Neville, C.J. Kepert, Angew. Chem. Int. Ed. 55 (2016) 15105–15109.
[114] J.E. Clements, J.R. Price, S.M. Neville, C.J. Kepert, Angew. Chem. Int. Ed. 53 (2014) 10164–10168.
[115] M. Paez-Espejo, M. Sy, K. Boukheddaden, J. Am. Chem. Soc. 138 (2016) 3202–3210.
[116] N.F. Sciortino, K.R. Scherl-Gruenwald, G. Chastanet, G.J. Halder, K.W. Chapman, J.F. Letard, C.J. Kepert, Angew. Chem. Int. Ed. 51 (2012) 10154–10158.
[117] I.A. Gural'skiy, B.O. Golub, S.I. Shylin, V. Ksenofontov, H.J. Shepherd, P.R. Raithby, W. Tremel, I.O. Fritsky, Eur. J. Inorg. Chem. (2016) 3191–3195.
[118] V. Niel, M.C. Muñoz, A.B. Gaspar, A. Galet, G. Levchenko, J.A. Real, Chem. Eur J. 8 (2002) 2446–2453.

[119] I.A. Gural'skiy, S.I. Shylin, B.O. Golub, V. Ksenofontov, I.O. Fritsky, W. Tremel, New J. Chem. 40 (2016) 9012–9016.
[120] J.Y. Li, Y.C. Chen, Z.M. Zhang, W. Liu, Z.P. Ni, M.L. Tong, Chem. Eur J. 21 (2015) 1645–1651.
[121] J.-Y. Li, Z.-P. Ni, Z. Yan, Z.-M. Zhang, Y.-C. Chen, W. Liu, M.-L. Tong, CrystEngComm 16 (2014) 6444–6449.
[122] Z.-P. Ni, J.-L. Liu, M.N. Hoque, W. Liu, J.-Y. Li, Y.-C. Chen, M.-L. Tong, Coord. Chem. Rev. 335 (2017) 28–43.
[123] X. Bao, H.J. Shepherd, L. Salmon, G. Molnár, M.L. Tong, A. Bousseksou, Angew. Chem. Int. Ed. 52 (2013) 1198–1202.
[124] R. Ohtani, M. Arai, A. Hori, M. Takata, S. Kitao, M. Seto, S. Kitagawa, M. Ohba, J. Inorg. Organomet. Polym. Mater. 23 (2013) 104–110.
[125] J.-Y. Li, C.-T. He, Y.-C. Chen, Z.-M. Zhang, W. Liu, Z.-P. Ni, M.-L. Tong, J. Mater. Chem. C 3 (2015) 7830–7835.
[126] K. Yoshida, D. Akahoshi, T. Kawasaki, T. Saito, T. Kitazawa, Polyhedron 66 (2013) 252–256.
[127] K. Hosoya, S.-i. Nishikiori, M. Takahashi, T. Kitazawa, Magnetochemistry 2 (2016) 8.
[128] Z. Arcís-Castillo, M.C. Muñoz, G. Molnár, A. Bousseksou, J.A. Real, Chem. Eur J. 19 (2013) 6851–6861.
[129] L. Piñeiro-López, Z. Arcís-Castillo, M.C. Muñoz, J.A. Real, Cryst. Growth Des. 14 (2014) 6311–6319.
[130] F.J. Muñoz-Lara, A.B. Gaspar, M.C. Muñoz, V. Ksenofontov, J.A. Real, Inorg. Chem. 52 (2013) 3–5.
[131] F.J. Muñoz-Lara, Z. Arcís-Castillo, M.C. Muñoz, J.A. Rodríguez-Velamazán, A.B. Gaspar, J.A. Real, Inorg. Chem. 51 (2012) 11126–11132.
[132] F.J. Valverde-Muñoz, M. Seredyuk, M.C. Muñoz, K. Znovjyak, I.O. Fritsky, J.A. Real, Inorg. Chem. 55 (2016) 10654–10665.
[133] J. Okabayashi, S. Ueno, Y. Wakisaka, T. Kitazawa, Inorg. Chim. Acta. 426 (2015) 142–145.
[134] T. Kitazawa, Y. Gomi, M. Takahashi, M. Takeda, M. Enomoto, A. Miyazaki, T. Enoki, J. Mater. Chem. 6 (1996) 119–121.
[135] O.I. Kucheriv, S.I. Shylin, V. Ksenofontov, S. Dechert, M. Haukka, I.O. Fritsky, I. y. A. Gural'skiy, Inorg. Chem. 55 (2016) 4906–4914.
[136] W. Liu, L. Wang, Y.-J. Su, Y.-C. Chen, J. Tucek, R. Zboril, Z.-P. Ni, M.-L. Tong, Inorg. Chem. 54 (2015) 8711–8716.
[137] J. Okabayashi, S. Ueno, T. Kawasaki, T. Kitazawa, Inorg. Chim. Acta. 445 (2016) 17–21.
[138] T. Kosone, T. Kitazawa, Inorg. Chim. Acta. 439 (2016) 159–163.
[139] E. Milin, V. Patinec, S. Triki, E.-E. Bendeif, S. Pillet, M. Marchivie, G. Chastanet, K. Boukheddaden, Inorg. Chem. 55 (2016) 11652–11661.
[140] N.F. Sciortino, F. Ragon, K.A. Zenere, P.D. Southon, G.J. Halder, K.W. Chapman, L. Piñeiro-López, J.A. Real, C.J. Kepert, S.M. Neville, Inorg. Chem. 55 (2016) 10490–10498.
[141] S.-L. Zhang, X.-H. Zhao, Y.-M. Wang, D. Shao, X.-Y. Wang, Dalton Trans. 44 (2015) 9682–9690.
[142] R. Herchel, Z. Trávníček, R. Zbořil, Inorg. Chim. Acta. 365 (2011) 458–461.
[143] F. Setifi, C. Charles, S. Houille, F. Thétiot, S. Triki, C.J. Gómez-García, S. Pillet, Polyhedron 61 (2013) 242–247.
[144] S.-i. Ohkoshi, K. Imoto, Y. Tsunobuchi, S. Takano, H. Tokoro, Nat. Chem. 3 (2011) 564–569.
[145] D. Pinkowicz, M. Rams, M. Mišek, K.V. Kamenev, H. Tomkowiak, A. Katrusiak, B. Sieklucka, J. Am. Chem. Soc. 137 (2015) 8795–8802.
[146] R.-M. Wei, M. Kong, F. Cao, J. Li, T.-C. Pu, L. Yang, X.-L. Zhang, Y. Song, Dalton Trans. 45 (2016) 18643–18652.
[147] E. Coronado, M. Giménez-Marqués, G. Mínguez Espallargas, F. Rey, I.J. Vitórica-Yrezábal, J. Am. Chem. Soc. 135 (2013) 15986–15989.
[148] N. Calvo Galve, E. Coronado, M. Giménez-Marqués, G. Mínguez Espallargas, Inorg. Chem. 53 (2014) 4482–4490.
[149] M. Weselski, M. Książek, J. Kusz, A. Białońska, D. Paliwoda, M. Hanfland, M.F. Rudolf, Z. Ciunik, R. Bronisz, Eur. J. Inorg. Chem. 2017 (2017) 1171–1179.
[150] A. Białońska, R. Bronisz, J. Kusz, M. Zubko, Eur. J. Inorg. Chem. 2013 (2013) 884–893.
[151] M. Seredyuk, L. Piñeiro-López, M.C. Muñoz, F.J. Martínez-Casado, G. Molnár, J.A. Rodriguez-Velamazán, A. Bousseksou, J.A. Real, Inorg. Chem. 54 (2015) 7424–7432.
[152] M. Ksiazek, J. Kusz, A. Bialonska, R. Bronisz, M. Weselski, Dalton Trans. 44 (2015) 18563–18575.
[153] J.-B. Lin, W. Xue, B.-Y. Wang, J. Tao, W.-X. Zhang, J.-P. Zhang, X.-M. Chen, Inorg. Chem. 51 (2012) 9423–9430.
[154] Y.-C. Chuang, C.-T. Liu, C.-F. Sheu, W.-L. Ho, G.-H. Lee, C.-C. Wang, Y. Wang, Inorg. Chem. 51 (2012) 4663–4671.
[155] W. Liu, X. Bao, J.-Y. Li, Y.-L. Qin, Y.-C. Chen, Z.-P. Ni, M.-L. Tong, Inorg. Chem. 54 (2015) 3006–3011.
[156] X. Bao, P.-H. Guo, W. Liu, J. Tucek, W.-X. Zhang, J.-D. Leng, X.-M. Chen, I. y. Gural'skiy, L. Salmon, A. Bousseksou, M.-L. Tong, Chem. Sci. 3 (2012) 1629–1633.
[157] F.-L. Yang, M.-G. Chen, X.-L. Li, J. Tao, R.-B. Huang, L.-S. Zheng, Eur. J. Inorg. Chem. 2013 (2013) 4234–4242.
[158] X.-R. Wu, H.-Y. Shi, R.-J. Wei, J. Li, L.-S. Zheng, J. Tao, Inorg. Chem. 54 (2015) 3773–3780.
[159] Y.-H. Luo, Q.-L. Liu, L.-J. Yang, Y. Ling, W. Wang, B.-W. Sun, J. Solid State Chem. 222 (2015) 76–83.
[160] J.A. Real, E. Andrés, M.C. Muñoz, M. Julve, T. Granier, A. Bousseksou, F. Varret, Science 268 (1995) 265–267.
[161] T. Romero-Morcillo, N. De la Pinta, L. M. Callejo, L. Piñeiro-López, M.C. Muñoz, G. Madariaga, S. Ferrer, T. Breczewski, R. Cortés, J.A. Real, Chem. Eur. J. 21 (2015) 12112–12120.
[162] C. Göbel, T. Palamarciuc, C. Lochenie, B. Weber, Chem. Asian J. 9 (2014) 2232–2238.
[163] O. Klimm, C. Gobel, S. Rosenfeldt, F. Puchtler, N. Miyajima, K. Marquardt, M. Drechsler, J. Breu, S. Forster, B. Weber, Nanoscale 8 (2016) 19058–19065.
[164] F. Shao, J. Li, J.-P. Tong, J. Zhang, M.-G. Chen, Z. Zheng, R.-B. Huang, L.-S. Zheng, J. Tao, Chem. Commun. 49 (2013) 10730–10732.
[165] T. Romero-Morcillo, F.J. Valverde-Munoz, M.C. Munoz, J.M. Herrera, E. Colacio, J.A. Real, RSC Adv. 5 (2015) 69782–69789.
[166] A. Lennartson, P. Southon, N.F. Sciortino, C.J. Kepert, C. Frandsen, S. Mørup, S. Piligkos, C.J. McKenzie, Chem. Eur J. 21 (2015) 16066–16072.
[167] S. Schonfeld, C. Lochenie, P. Thoma, B. Weber, CrystEngComm 17 (2015) 5389–5395.
[168] H.-Y. Wang, J.-Y. Ge, C. Hua, C.-Q. Jiao, Y. Wu, C.F. Leong, D.M. D'Alessandro, T. Liu, J.-L. Zuo, Angew. Chem. Int. Ed. 56 (2017) 5465–5470.
[169] R. Ohtani, K. Shimayama, A. Mishima, M. Ohba, R. Ishikawa, S. Kawata, M. Nakamura, L.F. Lindoy, S. Hayami, J. Mater. Chem. C 3 (2015) 7865–7869.
[170] K. Bhar, S. Khan, J.S. Costa, J. Ribas, O. Roubeau, P. Mitra, B.K. Ghosh, Angew. Chem. Int. Ed. 51 (2012) 2142–2145.
[171] S. Roy, S. Choubey, K. Bhar, N. Sikdar, J.S. Costa, P. Mitra, B.K. Ghosh, Dalton Trans. 44 (2015) 7774–7776.